Institut für Getriebetechnik, Maschinendynamik und Robotik

RWTH AACHEN UNIVERSITY

Diese Arbeit wurde vorgelegt am Institut für Getriebetechnik, Maschinendynamik und Robotik

# Development of Energy-efficient Dwell Mechanisms

Bachelorarbeit


*von:*

**B.Sc. Alfonso Baños Benítez**

Matrikelnummer: 447 988


*betreut von:*

Thomas Knobloch M.Sc. RWTH

*Prüfer:*

Univ.-Prof. Dr.-Ing. Dr. h. c. Burkhard Corves

Prof. Dr.-Ing. Mathias Hüsing

Aachen, den 08.09.2023

# Acknowledgements

This thesis has been conducted in the *Institut für Getriebetechnik, Maschinendynamik und Robotik* (IGMR) in RWTH Aachen, during my stay in this University through the ERASMUS exchange Program. I would like to acknowledge both my tutors, Thomas Knobloch in RWTH Aachen and Luis Baeza in my home university, *Universidad Politécnica de Valencia* (UPV). Their assistance and guiding in the elaboration of this work have been essential.

# Bachelorarbeit

*von* **B.Sc. Alfonso Baños Benítez**

*Matrikelnummer:* 447 988

**Development of Energy-efficient Dwell Mechanisms:**

In order to meet the goal of the Climate Protection Plan 2050 to limit global warming to 1.5°C, research is being undertaken in many industrial sectors to make machines, processes and technologies more energy efficient. One way to improve the efficiency is in machines that adopt dwell mechanisms, which are characterized by intermittent movements that alternate forward and backward displacements with holding positions. As a result of this function, there is unproductive energy consumption by the machine used to accelerate and stop the mechanism.

The main goal of this thesis is to investigate and develop methods to increase the energy efficiency of dwell mechanisms, focusing on the application of Eigenmotion. The different types and working principles of dwell mechanisms, focusing on 6-bar linkages, as well as the application of the Eigenmotion equations in this field must be studied. The theoretical background of dwell mechanism design will be researched to test the possibilities of designing a dwell mechanism of its own for this thesis.

Procedure:

1. Dwell mechanism research: Types and Fundamentals (State of the art)

2. Eigenmotion research (Introduction)

3. Design of a self-made Dwell Mechanism

4. Energy efficiency Study: Application of Eigenmotion to the designed Dwell Mechanism

5. Post-Eigenmotion Improvements: Studying possible output motion improvements for the efficient Dwell Mechanism

Betreuer: Thomas Knobloch M.Sc. RWTH

# Eidesstattliche Versicherung

Alfonso Baños Benítez Matrikelnummer:497 988

Ich versichere hiermit an Eides Statt, dass ich die vorliegende Bachelorarbeit mit dem Titel

**Development of Energy-efficient Dwell Mechanisms**

selbständig und ohne unzulässige fremde Hilfe erbracht habe. Ich habe keine anderen als die angegebenen Quellen und Hilfsmittel benutzt. Für den Fall, dass die Arbeit zusätzlich auf einem Datenträger eingereicht wird, erkläre ich, dass die schriftliche und die elektronische Form vollständig übereinstimmen. Die Arbeit hat in gleicher oder ähnlicher Form noch keiner Prüfungsbehörde vorgelegen.

Aachen, den 08.09.2023

Alfonso Baños Benítez

**Belehrung:**

**§ 156 StGB: Falsche Versicherung an Eides Statt**

Wer vor einer zur Abnahme einer Versicherung an Eides Statt zuständigen Behörde eine solche Versicherung falsch abgibt oder unter Berufung auf eine solche Versicherung falsch aussagt, wird mit Freiheitsstrafe bis zu drei Jahren oder mit Geldstrafe bestraft.

**§ 161 StGB: Fahrlässiger Falscheid; fahrlässige falsche Versicherung an Eides Statt**

(1) Wenn eine der in den §§ 154 bis 156 bezeichneten Handlungen aus Fahrlässigkeit begangen worden ist, so tritt Freiheitsstrafe bis zu einem Jahr oder Geldstrafe ein.

(2) Straflosigkeit tritt ein, wenn der Täter die falsche Angabe rechtzeitig berichtigt. Die Vorschriften des § 158 Abs. 2 und 3 gelten entsprechend.

Die vorstehende Belehrung habe ich zur Kenntnis genommen:

Aachen, den 08.09.2023

Alfonso Baños Benítez

**Table of contents**

## Formula Symbols and Indices

### *General symbols*

| | |
|---|---|
| $\dot{(\ )}$ | First derivative with respect to time |
| $\bar{(\ )}$ | Distance between two points |
| $\vec{(\ )}$ | Vector |
| const. | constant |

### *Latin small letters*

| | | |
|---|---|---|
| $m$ | mass | $[kg]$ |
| $v$ | speed | $[m \cdot s^{-1}]$ |
| t | time | $[s]$ |
| x | X coordinate | $[m]$ |
| y | Y coordinate | $[m]$ |

### *Latin capital letters*

| | | |
|---|---|---|
| $E$ | Energy | $[J]$ |
| $P$ | Power | $[W]$ |
| $T$ | Period | $[s]$ |
| $J$ | Mass moment of inertia | $[kg \cdot m^2]$ |

### *Greek small letters*

| | | |
|---|---|---|
| $\varphi$ | Crank angle | $[rad]$ |
| $\theta$ | Link angle (non-crank) | $[rad]$ |
| $\rho$ | Density | $[kg \cdot m^{-3}]$ |

### *Greek capital letters*

| | | |
|---|---|---|
| T | Torque | $[N \cdot m]$ |

### *Indices*

| | |
|---|---|
| *0* | Initial state |
| kin | Kinetic |
| pot | Potential |
| D | Drive |
| d | Drive unit |
| red | Reduced |
| e | Eigenmotion |
| max | Maximum |
| min | Minimum |
| i | Link |
| n | Total nº of links |
| CM | Mass center |
| T | Translational |
| ER | End rotation |
| CR | Center rotation |
| R | Rotational |

## List of Abbreviations

| | |
|---|---|
| IGMR | Institute of Mechanism Theory, Machine Dynamics and Robotics |
| GA | Genetic Algorithms |

# 1 Introduction

This thesis addresses two main issues. In the first place, dwell mechanisms are of interest because of their artful functioning and immeasurable applications in modern industry. In addition to this, Eigenmotion is of interest for its potential to improve energy efficiency in industrial processes, which meets environmental objectives of great importance at the present time. The following sections describe the different objectives and procedures derived from these areas of interest in this thesis.

## 1.1 Objectives

The overall goal of this thesis is to explore the relationship between dwell mechanisms and Eigenmotion. Therefore, this thesis is composed of two primary aims:

1. Theoretical: Undertaking a state-of-the-art literature research on dwell mechanisms, their functioning, and their possible design methods, as well as Eigenmotion.
2. Practical: Developing a self-made dwell mechanism and applying the Eigenmotion procedure to it. Obtaining an original dwell mechanism that can perform a desired motion while operating in Eigenmotion.

## 1.2 Procedure

After introducing the basics of mechanisms and Eigenmotion, the topic of dwell mechanisms and its different types are studied in more depth. Following this, a specific type of dwell mechanism is chosen for the application of Eigenmotion, according to the available criteria and information.

In this stage, the full design of a dwell mechanism of its own for this thesis is conducted. The working principles of dwell mechanisms as well as systematized methods of dwell mechanism design must be researched beforehand. A self-made dwell mechanism is then designed for this thesis, and Eigenmotion is applied to it. Following the initial application, further adjustments are made so that the output motion of the post-Eigenmotion mechanism matches that of the original one.

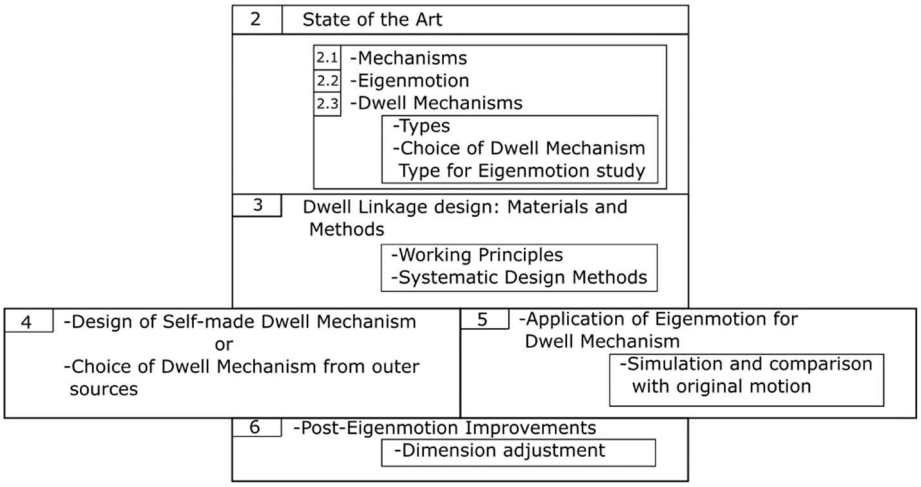


**Fig 1. 1**: Representation of the procedure, in reference to each section in the thesis.

# 2 State of the Art

As mentioned on section 1.1, the first aim of this thesis is undertaking a state-of-the-art literature research on the topics of interest for this thesis. The following sections present the different findings regarding dwell mechanisms and Eigenmotion, starting from the basics of mechanisms.

## 2.1 Introduction to Mechanisms

A useful working definition of a mechanism is "*a system of elements arranged to transmit motion in a predetermined fashion*". For a chosen element of reference, motion can refer to pure rotation, pure translation, or a combination of both [Nor99, S. 24]. This transmission of motion, which would develop low forces and transmit little power by itself, will enable transmissions of power of a much higher degree when integrated in machines along with other mechanisms [Nor99, S. 4].

The main goal of mechanism design can be described as successfully determining an output motion that performs a specific task. These tasks are defined by the specific requirements from processes that take place in a wide range of technological sectors [KCH15, S. 3]:

- Precision equipment technology
- Automotive engineering
- Textile engineering
- Packaging machines
- Printing technology
- Agricultural technology
- Stamping technology
- Cutting technology

Mechanisms can be divided into uniformly and non-uniformly transmitting mechanisms. Compared to the uniformly transmitting mechanisms, the transmission ratio of the non-uniformly translating mechanisms is not constant [Sch19, S. 21].

In transmission technology, a distinction is made between guiding and transmission mechanisms. In the latter, motion as well as power are transmitted to the output element. Guiding mechanisms are used to move a body as well as a mechanical element in or through defined positions or on defined guideways. This is referred to as the leading or guiding of mechanical elements [Sch19, S. 5–6].

An example of a transmission mechanism would be the reciprocating piston of the internal combustion engine. Here, the sliding movement of the reciprocating piston is converted into a rotating movement of the crankshaft is where the pushing motion of the reciprocating piston is converted into a rotating motion in the crankshaft (Fig. 2.1 (b)). A convertible top in an

automobile can serve as an example of guiding mechanisms: the top is brought from a fixed starting position to a defined end position via a guide track (Fig. 2.1 (a)) [Sch19, S. 5].

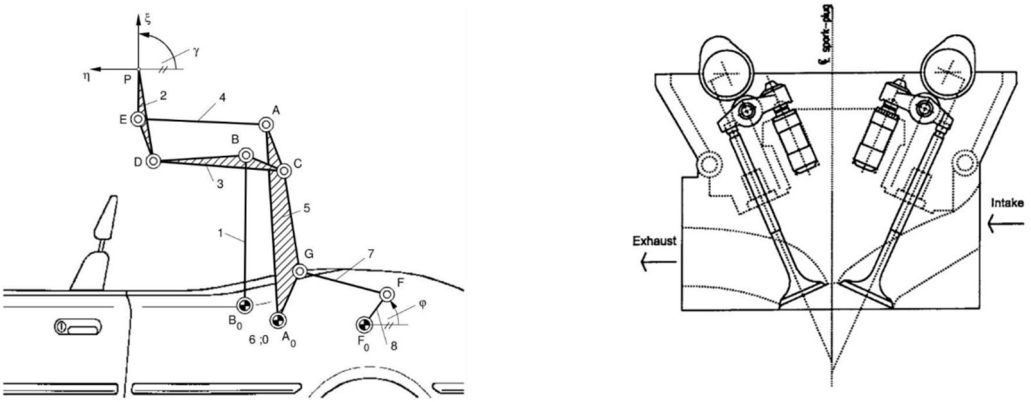


(a) **Convertible top** [Sto05]

(b) **Reciprocating piston in an internal combustion engine** [CLN02]

**Fig. 2. 1**: Examples of guiding (a) and transmission (b) mechanisms.

### 2.1.1 Linkage Mechanisms

Linkages are the basic building blocks of all mechanisms. All common forms of mechanisms (cams, gears, belts, chains) are in fact variations on a common theme of linkages. Linkages are made up of links and joints [Nor99, S. 24]:

- A link is an (assumed) rigid body which possesses at least two nodes, which are points for attachment to other links.
- A joint is a connection between two or more links (at their nodes), which allows some motion, or potential motion, between the connected links [Nor99, S. 25].

There are several types of joints, not all of which can be used in linkages. Using Reuleaux's classification of joints, linkages are mechanisms that only have lower pairs, that is, where there is surface contact between the joint elements (revolute joints). On the other hand, line or point contact between elemental surfaces characterizes higher pair joints, which connect a cam and its follower, for example [UPS17, S. 8].

Links will be classified as [Nor99, S. 28]:

- Crank: a link which makes a complete revolution and is pivoted to ground.
- Rocker: a link which has oscillatory (back and forth) rotation and is pivoted to ground.
- Coupler (or connecting rod): a link which has complex motion and is not pivoted to ground.

Ground is defined as any link or links that are fixed (nonmoving) with respect to the reference frame. Note that the reference frame may in fact itself be in motion [Nor99, S. 28].

Additionally, a fundamental characteristic of a linkage is its number of degrees of freedom (DOF): the number of inputs which need to be provided in order to create a predictable output, or the number of independent coordinates required to define its position [Nor99, S. 28], also known as the mobility of a linkage [UPS17, S. 12]. The number of DOF in a linkage is determined by its number of links and joints, with distinctions between the joint types. Different joints restrain the DOF of a mechanism in different ways [Nor99, S. 25]:

- Lower pairs, where there's surface contact (revolute joints), restrain 1 DOF (also called full joints)

- Higher pairs, where there's line/point contact (cam-follower joint), restrain 2 DOF (also called half joints)

For the determination of the number of DOF in a mechanism, Kutzbach's modification of Gruebler's equation (Eq. 2.1) can be used [Nor99, S. 29]. This is known as the Kutzbach criterion for the mobility of a planar n-link mechanism [UPS17, S. 8]:

$$M = 3 \cdot (L - 1) - 2 \cdot J_1 - J_2 \qquad \textbf{(2.1)}$$

Where:

- M: nº of degrees of freedom / mobility of the mechanism

- L: nº of links

- $J_1$: nº of 1 DOF (full) joints

- $J_2$: nº of 2 DOF (half) joints

A kinematic chain is defined as an assemblage of links and joints, interconnected in a way to provide a controlled output motion in response to a supplied input motion [Nor99, S. 27]. Kinematic chains or mechanisms may be either open or closed. In a closed chain, every link is connected to at least two other links, and they form one or more closed loops [UPS17, S. 7]. There are no open attachment points or nodes, and it may have one or more degrees of freedom. An open mechanism of more than one link always has more than one degree of freedom, thus requiring as many actuators (motors) as it has DOF. An open kinematic chain of two binary links and one joint is called a dyad [Nor99, S. 28].

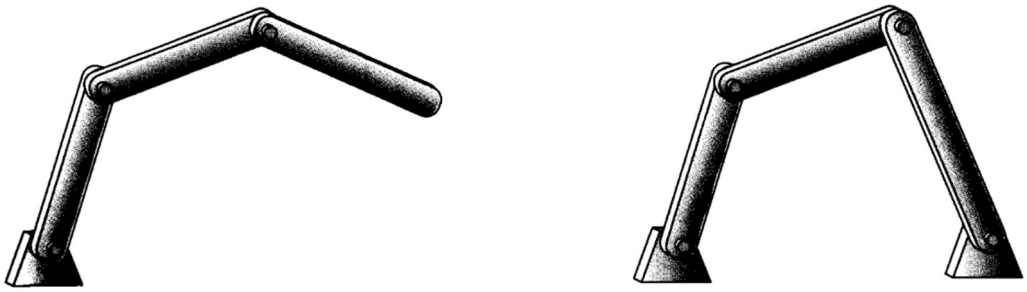

(a) **Open chain** (b) **Closed chain.**

**Fig. 2. 2**: Open and closed chain [Nor99, S. 29].

### 2.1.2 4-Bar Mechanisms

The 4-bar (or four-bar) mechanism is defined as the planar four-bar linkage, which has four links connected by four revolute pairs whose axes are parallel [UPS17, S. 12].

The four-bar linkage is the simplest possible pin-jointed mechanism for one-DOF mechanisms [Nor99, S. 46]. This can be explained using eq. (2. 1). If the Kutzbach criterion yields m = 1, the mechanism can be driven by a single input motion to produce constrained (uniquely defined) motion. Two examples are the slider-crank linkage and the four-bar linkage. From this equation, we see that a planar linkage with a mobility of m = 1 cannot have an odd number of links. Also, the simplest possible linkage with all binary links (two nodes per link) has $n = J_1 = 4$. This shows one reason why the four-bar linkage appears so commonly in machines [UPS17, S. 13].

The four-bar mechanism is also extremely versatile in terms of the types of motion it can generate. Due to this and its simplicity, it regarded as the most reliable and efficient solution to investigate motion control problems [Nor99, S. 46].

The rotation behavior of a four-bar linkage's inversions can be predicted via the Grashof condition, based only on the link lengths. Let:

S = length of shortest link L = length of longest link

P = length of one remaining link Q = length of another remaining link

Then if:

$$S + L \leq P + Q \quad \textbf{(2.2)}$$

At least one link will be capable of making a full revolution with respect to the ground plane. This is called a Class I kinematic chain. If the inequality is not true, no link will be capable of a complete revolution relative to any other link. This is a Class II kinematic chain. The possible motions from a four-bar linkage will depend on both the Grashof condition and the inversion chosen. An inversion is chosen by grounding (fixing) a different link in the kinematic chain [Nor99, S. 44]. There are as many inversions for a given linkage as there are links.

The inversions will be defined with respect to the shortest link. The motions are [Nor99, S. 48]:

- For the Class I case: $S + L < P + Q$
    - Ground either link adjacent to the shortest and you get a crank-rocker, in which the shortest link will fully rotate, and the other link pivoted to ground will oscillate.
    - Ground the shortest link and you will get a double crank, in which both links pivoted to ground make complete revolutions as does the coupler.
    - Ground the link opposite the shortest and you will get a Grashof double-rocker, in which both links pivoted to ground oscillate and only the coupler makes a full revolution.
- For the Class II case: $S + L > P + Q$
    - All inversions will be triple rockers in which no link can fully rotate.
- For the Class III case: S + L = P + Q

All inversions will be either double-cranks or crank-rockers but will have "change points" twice per revolution of the input crank when the links all become collinear. At these change points, the output behavior will become indeterminate. The linkage behavior is then unpredictable as it may assume either of two configurations. Its motion must be limited to avoid reaching the change points or an additional, out-of-phase link provided to guarantee a "carry through" of the change points.

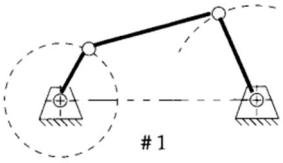


(a) **Crank Rocker Inversion (Example 1)**

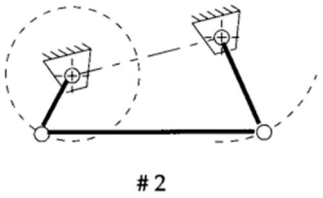


(b) **Crank Rocker Inversion (Example 2)**

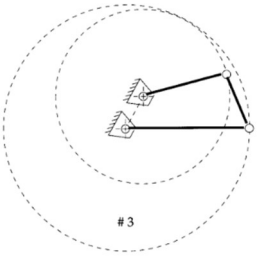


(c) **Double-crank inversion (drag link mechanism)**

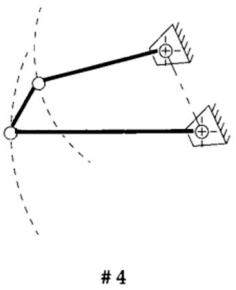


(d) **Double-rocker inversion (coupler rotates)**

**Fig. 2. 3**: All inversions of the Grashof four-bar linkage [Nor99, S. 46].

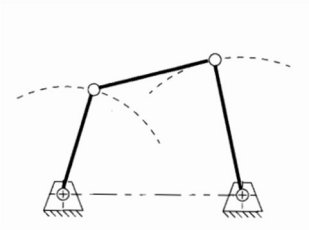

(a) **Triple Rocker #1**

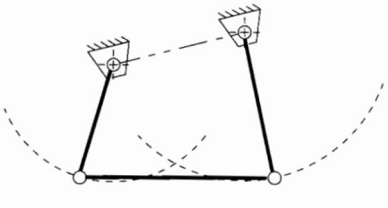

(b) **Triple Rocker #2**

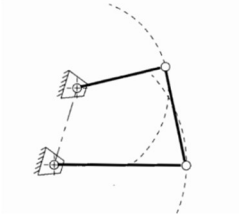

(c) **Triple Rocker #3**

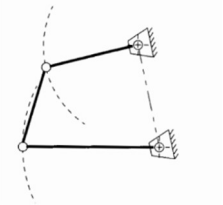

(d) **Triple Rocker #4**

**Fig. 2. 4**: All inversions of the non-Grashof four-bar linkage. It can be seen how they are all triple rockers [Nor99, S. 47].

## 2.2 Introduction to Eigenmotion

After introducing the basics of mechanism theory for this thesis, the topic of Eigenmotion is assessed. The following sections examine the reasons to research Eigenmotion, its definition and its basic equations.

### 2.2.1 Motivation for the study of Eigenmotion

In the last decades, there is a worldwide political and economic interest in increasing the environmental sustainability in industrial sectors, as it is expressed in international protocols and conventions. In the Kyoto Protocol, for example, sustainable development is promoted on a national scale through measures and policies such as [Uni98]:

- Enhancement of energy efficiency in relevant sectors of the national economy.
- Research on, and promotion, development and increased use of, new and renewable forms of energy, of carbon dioxide sequestration technologies and of advanced and innovative environmentally sound technologies.

"Energy efficiency" is defined by the EU Energy Efficiency Directive as the " the ratio of output of performance, service, goods or energy, to input of energy." Improving energy efficiency not only increases environmental sustainability (reduced greenhouse gas emissions, de-carbonization of the economy, improved air quality) but also reduces energy bills for industrial consumers, improving their competitiveness, and decreases energy imports, contributing to energy security [Eur15].

The “Climate and Energy Package 2030”, sets an energy efficiency improvement of at least 27% in EU countries as one of its key targets for 2030 [Eur16]. The evolution of energy efficiency targets for 2020 and 2030 are shown on Fig. 2.5.

In 2021, one of the industrial sectors with the highest energy consumption in Germany was the production and processing of metal. It is also one of the industries with the highest energy consumption in 2021 [Sta23]. This can be taken as an indicative that processing industry is a relevant sector in primary energy consumption in Germany.

The industrial sector represents more than one third of both global primary energy use [MPR07]. Therefore, improving the energy efficiency in production is a priority. For this reason, a decrease in power consumption is particularly important and correlates with the key EU target of increasing energy efficiency [Eur16].

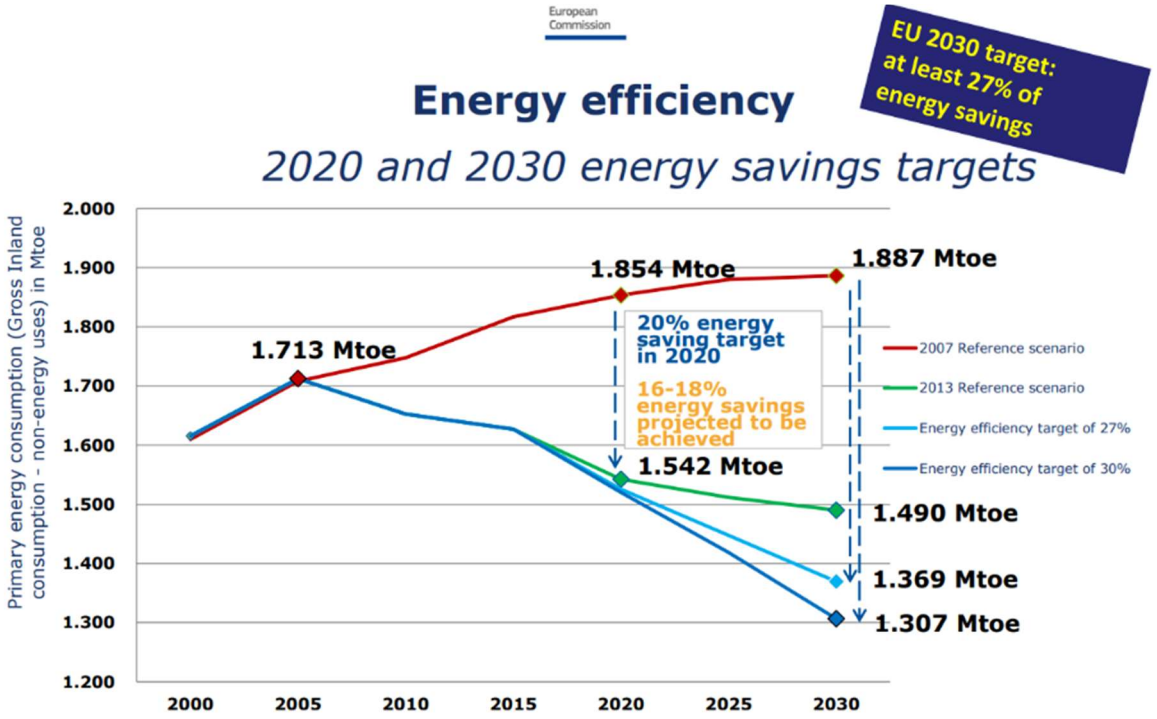


**Fig. 2. 5**: Evolution of EU energy efficiency targets for 2020 and 2030 [EC16, p. 11].

In a 2009 study by the Fraunhofer Institute for Introduction Systems and Innovation Research, the potential for energy savings in production in the manufacturing industry was estimated by the companies surveyed at an average of 15 % [SWB09]. Therefore, any procedure to increase the energy efficiency in the manufacturing industry is worth considering.

In the industrial sector, processing machines are commonly used. Their drive and control systems are of particular interest for energy saving. In the drive system, the electrical energy provided by the grid is converted into the form required for processing. Complex motion sequences are often required, which can be achieved using non-uniform transmission mechanisms driven by an electric motor with a constant drive speed. However, recent developments in the fields of control and drive technology allow the performance of these motion sequences using servomotors, which provide a non-constant drive speed. Together with the control system, which takes over the movement specification of the servo motor, the drive system forms the so-called movement system or motion system (MS) [Sch19, S. 2]. According to Callesen, one of the advantages of the motion system is the increase in energy efficiency (power equalization) [Cal08].

In this case, the increase in energy efficiency requires operating with a non-constant drive speed, which leads to the topic of Eigenmotion.

### 2.2.2 Definition of Eigenmotion

The concept of Eigenmotion is introduced through a sequence of equations. For plane mechanisms with a rotating input link (crank), the necessary drive power $P_D$ is the product of the drive torque $T_D$ and the input velocity $\dot{\varphi}$ [SHC17]:

$$P_D = T_D \cdot \dot{\varphi} \tag{2.3}$$

The drive torque can be written as follows [SC18]:

$$T_D = T_{Kin} + T_{pot} + T_{diss} + T_{proc} \tag{2.4}$$

$T_{Kin}$ is the necessary torque to overcome the resistances from accelerating and decelerating the links of the mechanism. $T_{pot}$ is the necessary torque to overcome the resistances resulting from gravity or springs. $T_{diss}$ and $T_{proc}$ include the resistances resulting from dissipation effects and process forces. The torque $T_{Kin}$ can be derived from the kinetic energy $E_{Kin}$ of the mechanism using the Lagrange Equations of 2nd kind [SC18; SHC17]:

$$T_{kin} = \frac{d}{dt}\left(\frac{\delta E_{kin}}{\delta \dot{\varphi}}\right) - \frac{\delta E_{kin}}{\delta \varphi} \tag{2.5}$$

Torque $T_{Kin}$ is null if the kinetic energy of the mechanism is constant. Eigenmotion refers to the specific motion of the crank that results in a constant kinetic energy of the mechanism over the whole period of motion, that is, where the torque required to overcome acceleration/deceleration resistances can be saved. Eq. (2.4) shows that driving a mechanism in its Eigenmotion can decrease the necessary input torque and result in a reduced energy consumption. Test benches have shown that operating mechanisms in their Eigenmotion increases their energy saving potential in comparison to constant motion speed [Sch19, S. 17].

### 2.2.3 Eigenmotion Formulation

After defining the concept of Eigenmotion, it will be formulated through a series of equations [SHC18].

Eigenmotion is the motion of a mechanism with M = 1 in case of a constant level of energy. The energy-level within the mechanism can be described by forming the sum of the kinetic energy $E_{kin}$ and the potential energy $E_{pot}$. In case of a constant level of energy in the system, eq. (2. 6) holds. Hereby, index '0' denotes the initial state.

$$E_{kin}(\varphi, \dot{\varphi}) + E_{pot}(\varphi) = const. = E_{kin}(\varphi_0, \dot{\varphi}_0) + E_{pot}(\varphi_0) \tag{2.6}$$

Introducing the reduced mass moment of inertia $J_{red}$ and a mass moment of inertia $J_d$, comprising the mass moment of inertia of the drive unit, eq. (2. 6) can be reformulated:

$$\frac{(J_{red}(\varphi)+J_d)}{2}\cdot\dot{\varphi}^2+E_{pot}(\varphi)=\frac{(J_{red}(\varphi_0)+J_d)}{2}\cdot\dot{\varphi}_0{}^2+E_{pot}(\varphi_0) \tag{2.7}$$

Solving eq. (2.7) for the input angular velocity, the following equation can be derived:

$$\dot{\varphi}_e=\sqrt{\frac{(J_{red}(\varphi_0)+J_d)\cdot\dot{\varphi}_0{}^2+2E_{pot,0}-2E_{pot}(\varphi)}{J_{red}(\varphi_e)+J_d}} \tag{2.8}$$

The Eigenmotion of the mechanism refers to this specific crank velocity. The Eigenmotion (index ‘e’) describes a certain motion of the mechanism, which can be expressed in terms of different links of the mechanism and with respect to their position, velocity and acceleration. In order to sustain the full revolution of the input link (crank), the radicand in eq. (2.8) has to be positive.

Considering that only the maximum of the potential energy is relevant, an equation for the minimum initial angular velocity can be derived:

$$\dot{\varphi}_{0,min}=\sqrt{\frac{2\cdot\left(max\left(E_{pot}(\varphi)\right)-E_{pot}(\varphi_0)\right)}{J_{red}(\varphi_0)+J_d}} \tag{2.9}$$

In order to derive the trend of the crank position in Eigenmotion, eq. (2.9) can be reformulated as follows:

$$d\varphi_e=\sqrt{\frac{(J_{red}(\varphi_0)+J_d)\cdot\dot{\varphi}_0{}^2+2E_{pot,0}-2E_{pot}(\varphi)}{J_{red}(\varphi_e)+J_d}}\,dt \tag{2.10}$$

The period of the Eigenmotion can then be derived from this equation by integration:

$$T_e=\int_{\varphi_0}^{\varphi_0+2\pi}\sqrt{\frac{J_{red}(\varphi_e)+J_d}{(J_{red}(\varphi_0)+J_d)\cdot\dot{\varphi}_0{}^2+2E_{pot,0}-2E_{pot}(\varphi)}}\,d\varphi \tag{2.11}$$

These are the basic equations of Eigenmotion. The topic of Eigenmotion is set apart in the following sections to introduce dwell mechanisms.

## 2.3 Introduction to Dwell Mechanisms

In some cases, the processes in the technological sectors mentioned in Section 2. 1 require the output motion of a mechanism to stop and stay still for some time (dwell). Norton defines the dwell as "*zero output motion for some nonzero input motion.*" Even though the motor keeps working as before, the output motion stays still for a time period [Nor99, S. 125]. Mechanisms that perform this effect are called dwell mechanisms, and they can be applied to fulfill a wide variety of functions which can be enumerated as follows:

Some interruptions are required for time-dependent work steps, such as the heat input during sealing processes, or film copiers [KCH15, S. 271]. Any production step where a tool is fed into a workspace and held there while some other task is performed [Nor99, S. 125], in textile production processes, for example. Guiding or transmission mechanisms (Fig. 2. 1), like the roof of a convertible car, or the valve train in a combustion engine [CLN02]. Inside a packaging machine, it may be necessary to connect an input shaft and an output shaft so that the output shaft oscillates with a prescribed dwell period and timing while the input shaft rotates continuously [SE84, S. 231]. A valve in an automotive engine must open, remain open for a brief time period, and then close. A conveyor line may need to halt for an interval of time while an operation is being performed and then continue its motion [UPS17, S. 29].

This functional field has also been synthetized as two encompassing functions [Nor99]:

- Allowing the loading or delivery of a part.
- Allowing other events to complete during a process.

However, the wide variety of requirements and motion transmissions can make the mechanism design process seem chaotic if a more heuristic or systematized approach is not available. It would be an ideal situation if a designer could consult a system with his own list of specifications and obtain a list of mechanisms to satisfy them [UPS17, S. 17]. In *A Thesaurus of Mechanisms*, Torfason outlines a classification of mechanisms based on different types of motion transmission, where a thoughtful introduction to Dwell Mechanisms has been found.

Under the category "Stops, Pauses and Hesitations", Torfason gathers machine elements (mechanisms) that cause an output "to stop and dwell, to stop and return, to stop and advance, etc.". The derivatives of the motion at the stop determine which category the motion fits. These functions are shown on Fig. 2. 6:

(a) **Geneva stops**

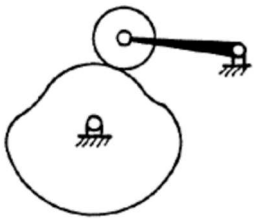

(b) **Cams**

(c) **Linkage at extreme limits**

(d) **Combinations of linkages at a limit #1**

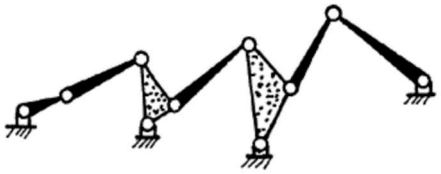

(e) **Combinations of linkages at a limit #2**

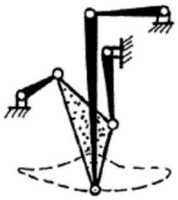

(f) **Outputs required from coupler curves #1**

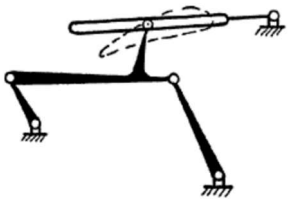

(g) **Outputs required from coupler curves #2**

**Fig. 2. 6**: Mechanisms assembled under the category "Stops, Pauses and Hesitations" in "A Thesaurus of Mechanisms" [Tor04].

From this assemble of mechanisms, the variety of mechanisms that can perform a dwell are narrowed down. Here it is useful to mention the definition of a mechanism by Reuleaux: "*Assemblage of resistant bodies, connected by movable joints, to form a closed kinematic chain with one link fixed and having the purpose of transforming motion*." With the help of this definition, the mechanisms of interest for this thesis can be further described by the following conditions [UPS17, S. 6–11]:

- Composed of rigid elements (links), that is, where no relative motion takes place between two randomly chosen points in the same link. Links are connected to each other by joints.

- The fixed link is used as a reference for the motions of all the other links in the mechanism.

- A fixed joint, which the fixed link is connected to, is also the point through which the input motion is introduced, via an axis connected to an engine. This joint is the driver. A chosen non-fixed joint, called the driven, follower or output, will move along the resulting output motion, which can be visualized as drawing an often-irregular curve.

- Planar mechanisms: All points in the mechanism describe curves parallel to a single common plane, therefore the motion transformation is coplanar. This allows the motion of any point belonging to the mechanism to be drawn in its true size and shape.

Those mechanisms in Torfason's assemble (Fig. 2. 6) where the output motion returns or advances after the stop can be ruled out, that is, "Geneva crosses" (a), "linkage at extreme limit" (c). The remaining mechanisms can be used to perform dwells: "cams" (b), "outputs required from coupler curves" (f) and "combinations of linkages at a limit" (d, e)

### 2.3.1 Types of dwell mechanisms

The types of mechanisms capable of performing dwells will be further evaluated. These are cams and linkages. The linkage section will focus on the coupler curve definition and properties, which would correspond to "outputs required from coupler curves" in Fig. 2. 6. Dwell mechanisms derived from "combinations of linkages at a limit" will be further explained in section 2.4.1.2.

#### 2.3.1.1 Cams

A cam is a machine element used to drive another element, called a follower, through a specified output motion by direct contact [UPS17, S. 298]. The cam has an irregular profile shape which can be described as a circle with a series of different diameters stemming from its center of rotation. As the cam rotates around itself, the follower will be lifted or pulled down due to the increase or decrease in the cam diameter, and it will dwell in those sections where the cam diameter is constant, as seen in Fig. 2. 7:

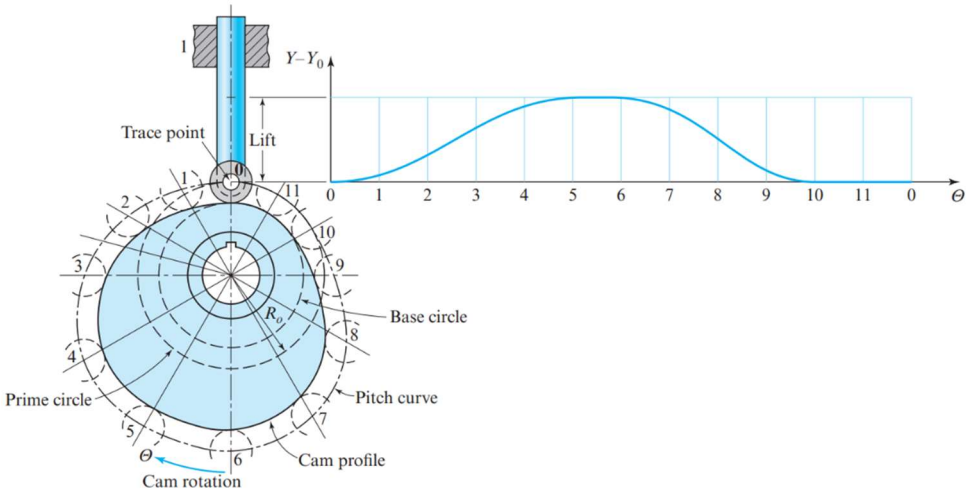


**Fig. 2. 7**: Representation of a cam-follower mechanism including its terminology and output motion curve, where a dwell can be seen between positions 5 and 6 [UPS17, S. 304].

Virtually any desired output function can be specified by creating a curved surface on the cam to generate that function in the motion of the follower [Nor99, S. 345]. Cam-and-follower mechanisms are simple and inexpensive, have few moving parts, and occupy very little space. Furthermore, follower motions having almost any desired characteristics are not difficult to design. For these reasons, cam mechanisms are used extensively in modern machinery [UPS17, S. 298], as guiding or transmission mechanisms. The synthesis of cam mechanisms includes the determination of the cam dimensions and the calculation of its curvature [CLN02], which will be of importance when the possibilities of studying Eigenmotion in dwell mechanisms are considered.

#### 2.3.1.2 Linkages: Outputs required from coupler curves

The coupler of a four-bar mechanism may be imagined as an infinite plane extending in all directions but pin-connected to the input and output cranks. During the linkage motion, any point attached to the plane of the coupler generates a path with respect to the fixed link; this path is called a coupler curve. All linkages that possess one or more coupler links will generate coupler curves [Nor99, S. 103]. Two of these paths, namely those generated by the pin connectors of the coupler, are true circles with centers at the two fixed pivots. However, other points can be found that trace much more complex curves [UPS17, S. 29]. In general, the more links, the higher the degree of curve generated, where degree means the highest power of any term in this equation. The four-bar slider-crank has, in general, fourth degree coupler curves, while the pin-jointed four-bar has up to sixth degree coupler curves [Nor99, S. 103].

Two examples of coupler curves for 4-bar linkages can be seen on Fig. 2. 8. On Fig. 2. 8 (a), there is a movie camera film-advance mechanism. It consists of a 4-bar mechanism where the coupler is extended until the point C, which is in contact with the film. The coupler curve of

this point can be seen, as well as the motion curve of points A (crank motion) and B (rocker motion) [Nor99, S. 107]. On Fig. 2. 8 (b), there is a 4-bar mechanism with a triangular coupler link, where the coupler curve traced by point P is shown. Link 2 is the crank and link 4 is the rocker [UPS17, S. 88].

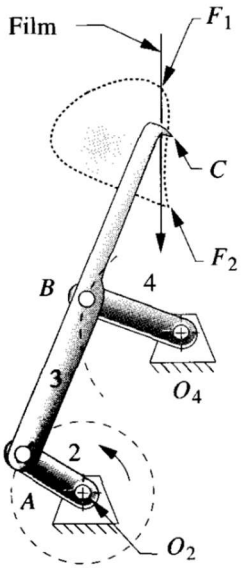


(a) **Movie Camera film-advance mechanism]** [Nor99, S. 107]**.**

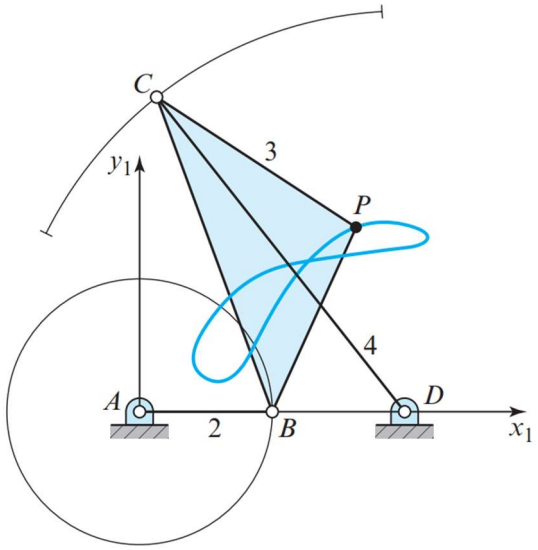


(b) **4-bar mechanism with a triangular coupler link** [UPS17, S. 88]**.**

**Fig. 2. 8**: Examples of coupler curves in 4-bar linkage mechanisms.

Coupler curves can be used to generate useful path motions for machine design problems. Coupler curve segments that approximate circular and straight-line segments can be exploited to generate dwell motions by adding two extra links, thus creating a six-bar dwell linkage mechanism [KCH15; Nor99; UPS17], as can be seen on Fig. 2. 9. Different methods for dwell linkage design will be evaluated on further sections, since there are different working principles for dwell motions in linkages that require further evaluation.

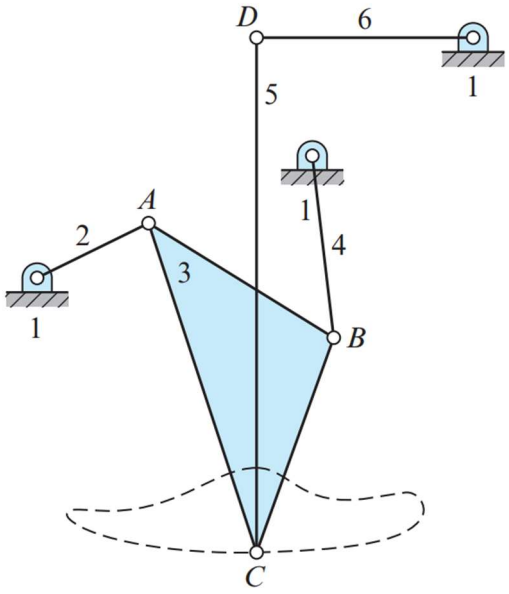


**Fig. 2. 9**: A 6-bar dwell linkage mechanism with an approximately circular coupler curve segment [UPS17, S. 29].

A useful reference for this method of dwell motion design is the *Analysis of the Four-Bar Linkage* by Hrones & Nelson, also known as the "Atlas of four-bar coupler curves" [HN51]. It contains around 7000 coupler curves, defining the linkage geometry for each of its Grashof crank-rocker linkages, using the crank length as the unit. The coupler includes fifty coupler points for each linkage geometry, arranged ten to a page. Therefore, approximate straight linear or circular coupler curve segments can be easily found.

Fig. 2. 10 shows a page of the H&N atlas page. The double circles indicate the fixed joints. The crank is always of unit length. The ratios of the other link lengths in reference to the crank are shown on each page. The real link lengths can be scaled up or down, this will affect the dimensioning of the linkage but not the shape of its coupler curve. Any of the coupler points shown can be used by incorporating it into a triangular coupler link.

The coupler curves in the H&N Atlas are shown as dashed lines. Each dash station represents five degrees of crank rotation. So, for an assumed constant crank velocity, the dash spacing is proportional to path velocity. The changes in velocity and the quick-return nature of the coupler path motion can be clearly seen from the dash spacing. One can peruse this linkage atlas resource and find an approximate solution to virtually any path generation problem. Then one can take the tentative solution from the atlas to a CAE simulator such as and further refine the design, based on the analysis of positions, velocities, and accelerations provided by the program [Nor99, S. 105]. In this thesis, IGMR planar mechanism design software Mechdev can be used for this goal.

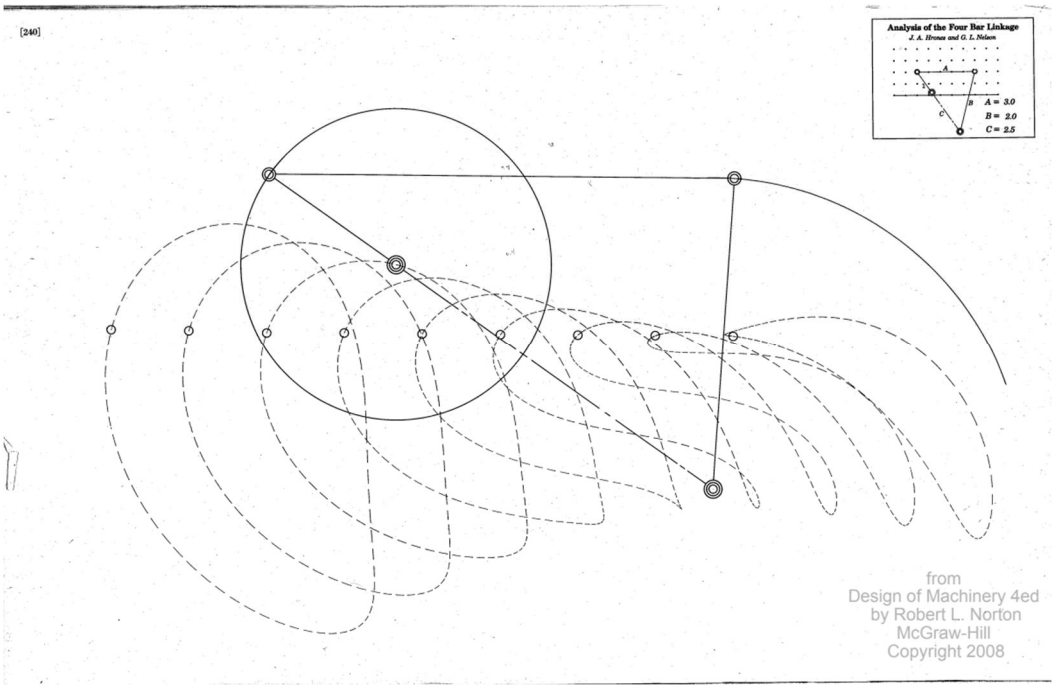


**Fig. 2. 10**: A page of the H&N Atlas of Coupler Curves, where a 4-bar crank-rocker linkage with defined dimensional proportions is shown along with coupler curves for different points that can be connected to its coupler link [HN51, S. 240].

### 2.3.2 Choice of the Dwell Mechanism Type

After conducting an overview of the 2 types of mechanisms from which dwell output motions can be derived, one of them must be chosen to study its possibilities in energy efficiency increase through Eigenmotion.

According to Norton, the "pure" revolute-jointed linkage with good bearings at the joints is a potentially superior design, all else equal, and it should be the first possibility to be explored in any machine design problem [Nor99, S. 59]. However, there will be many problems in which the need for a straight, sliding motion or the exact dwells of a cam-follower are required. The respective advantages and disadvantages of linkages and cam-follower mechanisms are shown in Tab. 2.1.

**Tab. 2. 1:** Advantages and disadvantages of the use of Linkages and Cam-follower Mechanisms [Nor99, S. 59–60; UPS17, S. 297]**.**

| Type of mechanism | Advantages | Disadvantages |
|---|---|---|
| Linkage | • Much easier and cheaper to manufacture to high precision than cams.<br>• Endurance in very hostile environments with poor lubrication.<br>• Better high-speed dynamic behavior<br>• Smaller sensitivity to manufacturing errors<br>• High load endurance | • Relatively large size compared to the output displacement of the working portion.<br>• More difficult to package.<br>• Relatively difficult to synthesize.<br>• More difficult dwell obtention.<br>• Less accurate dwell motion |
| Cam-Follower | • Compact in size compared to the follower displacement.<br>• Relatively easy to design (if computer tools are available)<br>• Easier dwell obtention<br>• More accurate dwell motion<br>• Better match to specified output motions | • No endurance in hostile environments, unless it's sealed from environmental contaminants |

A clear answer is not easily found since each option brings its own advantages and drawbacks [UPS17, S. 297]. Norton advises, "Because of the potential advantages of the pure linkage it is important to consider a linkage design before choosing a potentially easier design task but an ultimately more expensive solution" [Nor99, S. 60]. This can be taken as an economic advantage for linkages.

Additionally, the process characteristics intrinsic to the application of Eigenmotion to a mechanism must be considered. Eigenmotion requires a kinematical analysis of a mechanism, which can be expressed more comfortably through the derivation of vector position equations from a kinematic chain system. However, studying the energy efficiency possibilities of a cam-follower mechanism requires handling more abstract curvature and dimension variables. Therefore, choosing linkages for the study of Eigenmotion is seen as the best option, even if it requires a harder dwell obtention and design process.

## 2.4 Dwell Linkage Design

After deciding to study dwell linkages, two options are presented:

- Choosing a "ready-made" dwell linkage from available literature or internet sources and beginning the Eigenmotion study.
- Researching different ways to design a dwell linkage from the beginning, so that its exact output motion can be chosen.

The first option is found easier, but it doesn't provide substantial knowledge about the inner workings of dwell linkages, or about how they're really designed. The second option requires studying the available dwell linkages and understanding their working principles, so that a possible design method can be derived from them. This would enable an intentional choice of the dwell motion that can be obtained with a dwell, which would be of interest for practical purposes in dwell linkage design. Therefore, the second option is chosen.

### 2.4.1 Dwell Linkages: Working Principles Overview

In order to be able to design a dwell linkage, it must be understood how existing dwell mechanisms work.

#### 2.4.1.1 6-Bar Linkages: 4-bar + Dyad

As mentioned earlier, the four-bar chain is the basic building block of one-DOF mechanisms. However, the 4-bar linkage can produce flexible sinusoidal outputs, but it cannot produce dwells of useful duration. Furthermore, its limited force-transmission efficiency is also restricting [SE84, S. 298]. As mentioned on section 2.3.1.2, one way to obtain dwells in the output motion of a four-bar linkage is adding a dyad (two links) by connecting it to the coupler point [ KCH15; Nor99; UPS17;].

Fig. 2.11. shows how dyads can produce a dwell motion for different coupler curve geometries. These coupler curves would be traced by unseen 4-bars, which the dyads would be connected to. In the first case (a), an approximately elliptic coupler curve is chosen from the H&N Atlas. This coupler curve has a constant radius arc segment. Connecting link 5 is given a length equal to the radius of this arc. Thus, points D1, D2, and D3 are stationary as coupler point C moves through the arc segment (positions C1-C2-C3). Therefore, link 6 dwells in this position (1-2-3) before starting to move again towards position 4. In the second case (b), a coupler curve with a straight-line segment is chosen. Using a dyad with a slider joint, link 6 dwells as point C traces the straight-line segment. In this case one can speak of "constant angle" in the dwell producing link. It is important to note that the straight-line segment must be oriented towards the fixed joint ($O_6$) [KCH15, S. 272].

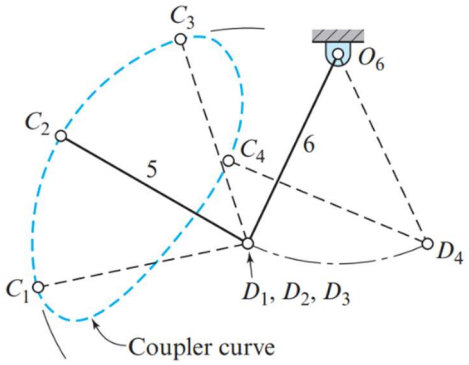


(a) **Dyad dwells during a circular coupler curve arc.**

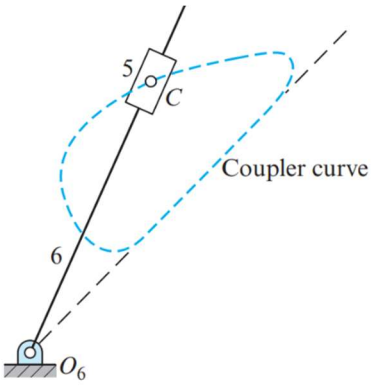


(b) **Dyad dwells during a straight-line coupler curve segment**

**Fig. 2. 11**: Examples of different dwell motions for dyads that follow coupler curves with different geometries: circular arc (a) and straight-line segment (b). These coupler curves would be traced by 4-bar linkages which are not shown [UPS17, S. 499].

#### 2.4.1.1.1 Single Dwell Linkages

From these two cases analyzed in Fig. 2. 11, 2 working principles for dwell obtention via 6-bar linkages can be derived [KCH15, S. 272]:

- Coupler curve sections with approximately constant radius.
- Coupler curves with approximately straight-line segments.

When 2-link gears (dyads) are added to the coupler points of 4-bar linkages that trace these types of coupler curves, the output members of the dyads will perform dwells. The duration of these dwells, measurable by its occupation in the input crank cycle, depends on the exact shape of each coupler curve [HN51; Nor99]. Therefore, the H&N Atlas of Coupler Curves is necessary for the obtention of dwells. Linkages such as the Watts-2 and Stephenson-3 on Fig. 2.12. can be used for this end [KCH15, S. 272]. Symmetrical coupler curves are also well suited to this task [Nor99, S. 126].

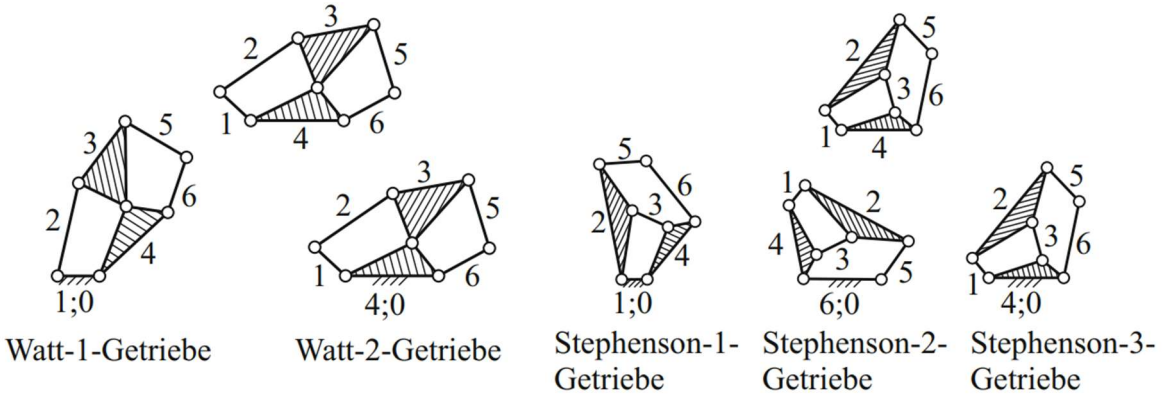


(a) **Watt's kinematic chain and linkages derived from it**

(b) **Stephenson's kinematic chain and linkages derived from it**

**Fig. 2. 12**: Planar six-bar crank linkages [KCH15, S. 272].

Further examples of linkages with straight-line coupler curve segments for the obtention of single dwells are shown on Fig. 2. 13.:

- Cases (a), (b): an additional couple of links (dyad) with a sliding joint is required for obtaining a dwell output motion [KCH15, S. 42].
- Case (c), Coupler curve-based linkage with 6 revolute joints and 1 sliding joint (approximate straight line) [KCH15, S. 273].
- Case (d): The slider mechanism uses a figure-eight coupler curve having a straight-line segment to produce an intermediate dwell linkage. Pivot O6 must be located on an extension of the straight-line segment, as shown [UPS17, S. 500].

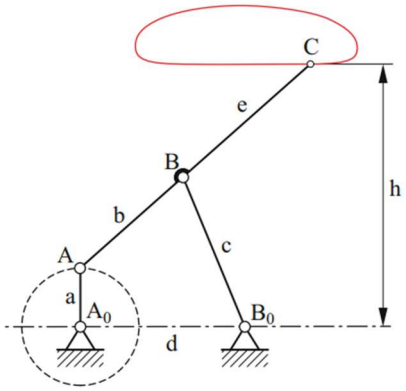


(a) **4-bar linkage tracing a coupler curve with horizontal straight line segment** [KCH15, S. 42]**.**

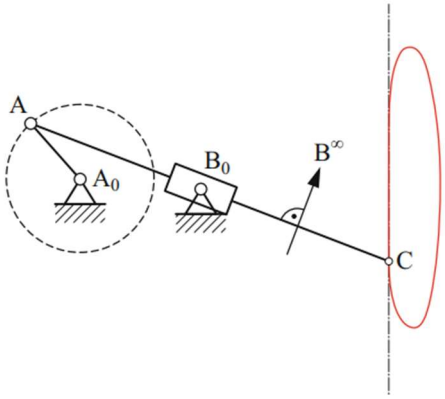


(b) **4-bar linkage tracing a coupler curve with vertical straight line segment** [KCH15, S. 42].

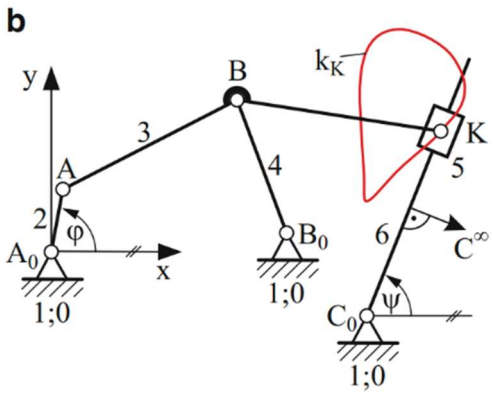


(c) **6-bar linkage with slider joint tracing a coupler curve with a straight line segment** [KCH15, S. 273].

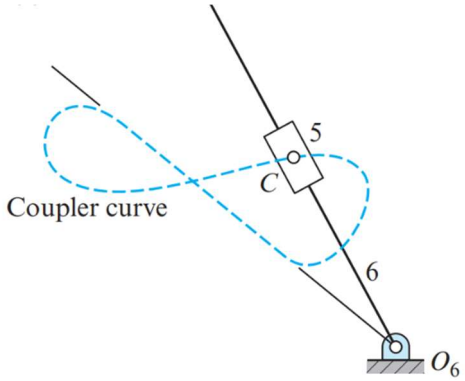


(d) **Dyad with slider joint tracing a "figure-eight" coupler curve with a straight line segment** [UPS17, S. 500].

**Fig. 2. 13**: Further examples of mechanisms tracing coupler curves with straight line segments.

#### 2.4.1.1.2 Double Dwell Linkages

It is also possible, using a four-bar coupler curve, to create a double-dwell output motion. Coupler curves suitable for double dwells are divided in two categories [Nor99, S. 128]: double circle arcs and double straight line segments.

Regarding double circle arcs (Fig. 2.14. and Fig. 2.15.), the coupler curve has two approximate circle arcs of the same radius but with different centers, both convex or both concave. A link 5 of length equal to the radius of the two arcs will be added such that it and link 6 will remain nearly stationary at the center of each of the arcs, while the coupler point traverses the circular parts of its path. Motion of the output link 6 will occur only when the coupler point is between those arc portions [Nor99, S. 128].

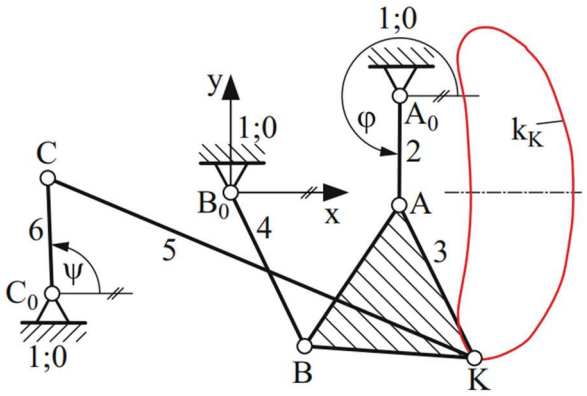


**Fig. 2. 14**: Double dwell linkage with 7 revolute joints (approximately constant radius of curvature) [KCH15, S. 273].

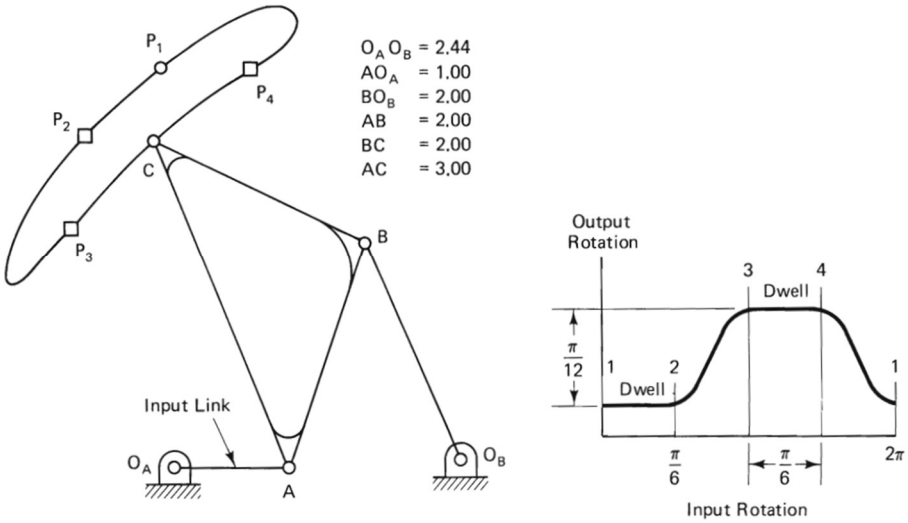


**Fig. 2. 15**: 4-bar linkage traces a symmetric, double dwell coupler curve [SE84, S. 269].

In the case shown in Fig. 2. 15, the coupler curve provides two arc sections in the position intervals (1-2) and (3-4). Through the addition of a dyad with an arc-diameter-long 5$^{th}$ link, the double-dwell output rotation displayed on the right side of the figure can be obtained.

The other double dwell case consists of coupler curves that contain two approximate straight-line segments of appropriate duration (Fig. 2. 16). If a pivoted slider block (link 5) is attached to the coupler at this point (C), and link 6 is allowed to slide in link 5, it only remains to choose a pivot $O_6$ at the intersection of the extended straight-line segments. While link 5 is traversing the "straight-line" segments of the curve, it will not impart any angular motion to link 6 [UPS17, S. 500]. The approximate nature of the four-bar straight line also causes some jitter in these dwells [Nor99, S. 128–129].

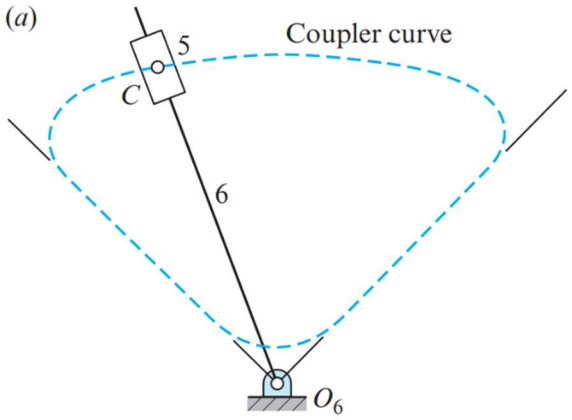


**Fig. 2. 16**: This arrangement has a dwell at both motion ends of link 6. A practical design of this mechanism may be difficult to achieve, however, since link 6 has a high velocity when the slider is near the pivot, $\boldsymbol{O_6}$ [UPS17, S. 500].

### 2.4.1.2 Combination of 2 4-bar Linkages

Another functional principle for dwell linkages is based on the connection of two four-bar linkages by utilizing their dead positions. If one combines the two sub-gears in such a way that the output member of the first sub-gear becomes the input member of the second sub-gear (Fig. 2.17), this is called “multiplicative coupling” [KCH15, S. 273–274].

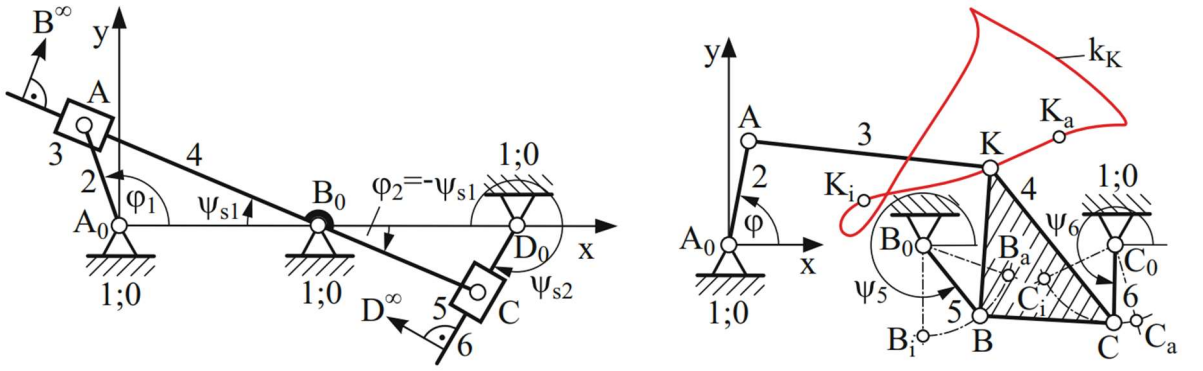


(a) **Oscillating dwell linkage**

(b) **Coupler curve-based dwell linkage of the 2nd type**

**Fig. 2. 17**: Coupler curve-based dwell linkages with multiplicative coupling [KCH15, S. 273].

In the case of the so-called oscillating dwell linkage (Fig. 2.17. (a)), this happens when the lengths $l_2 = \overline{A_0A}$ as well as $l_6 = \overline{D_0C}$ are perpendicular to $l_4 = \overline{B_0A}$ or $\overline{B_0C}$. If $A_0AB_0$ and $B_0CD_0$ also form similar triangles, there is a linkage with two identical dwells and a point symmetrical transfer function of the 0th order. In the case of the gear in Fig. 2.17 (b), a four-bar linkage is driven via a two-bar linkage attached to the coupling point K and not vice versa, as usual. Such mechanisms are referred to as coupler curve-based dwell linkages of the 2nd type. This gear also has two possible output links; $l_5$ and $l_6$, each of which performs two dwells [KCH15, S. 274].

# 3 Dwell Linkage Design: Materials and Methods

After studying the working principles of dwell linkages and classifying them according to their different output motions (single/double dwell, straight line/arc segment) and configuration (6-bar/pair of 4-bars), more detailed design processes will be studied. It is a decisive part for this thesis, because it is intended to find a systematic way to develop a dwell linkage mechanism from the start. After overviewing the available methods, one method will be chosen to finally design the dwell mechanism for this thesis.

Even though not all methods are systematized to the same detail, they all start at the same initial position: Consulting the H&N Atlas of Coupler Curves and choosing a fitting curve.

### 3.1.1.1 Overlay

A brief method for 6-bar dwell design is offered in *Theory of Machines and Mechanisms* [UPS17, S. 499–500]. A coupler curve having an approximately elliptic shape (single arc segment) is selected from the H&N Atlas so that a substantial portion of the curve approximates a circular arc. Connecting link 5 is given a length equal to the radius of this arc.

The overlay (Fig. 3.1) is done using a sheet of tracing paper and can be used when circular arcs in coupler curves are desired. It can be fitted over the paths in the H&N Atlas very quickly. For a case like the one shown in Fig. 2.11 (a), it quickly reveals the radius of curvature of the segment, the location of pivot point D and the displacement angle of the connecting link. Therefore, the main geometrical properties of the dyad can be determined by the overlay.

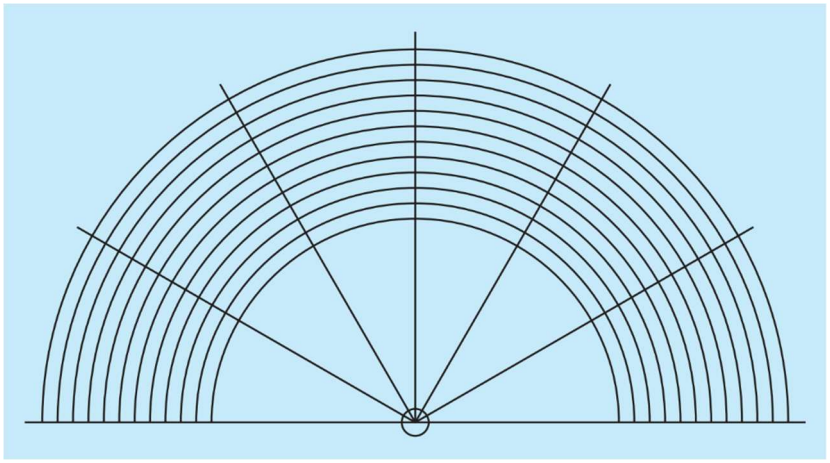

**Fig. 3. 1**: Overlay for use along with the H&N Atlas [UPS17, S. 499].

This contribution, however, is only useful for designing 6-bar dwell mechanisms given a circular coupler curve segment, and it does not explain how to build the whole linkage mechanism on a deeper level, or which variables can be adjusted by the dyad properties left to the designer's will.

#### 3.1.1.2 Double straight-line dwell linkage design

A complete design process for a 6-bar double dwell linkage based on a coupler curve with 2 straight line segments is proposed in Design of Machinery [Nor99, S. 129–130]. The following motion properties can be adjusted:

- Rocker-crank output motion relationship
- 1st dwell motion angle in crank cycle
- Return crank motion angle
- 2nd dwell motion angle in crank cycle

In this case, a full design process is described step by step for a six-bar linkage with a 80º rocker output motion over 20 crank degrees with dwell for 160º, return motion over 140º and second dwell for 40º.

1. Search the H&N atlas for a four-bar linkage with a coupler curve having two approximate straight-line portions. One should occupy 160º of crank motion (32 dashes), and the second 40º of crank motion (8 dashes). This is a wedge-shaped curve as shown in Fig. 3.2. (a).

2. Lay out this linkage to scale including the coupler curve and find the intersection of two tangent lines collinear with the straight segments. Label this point $O_6$.

3. Design link 6 to lie along these straight tangents, pivoted at $O_6$. Provide a slot in link 6 to accommodate slider block 5 as shown in Fig. 3. 2. (b).

4. Connect slider block 5 to the coupler point P on link 4 with a revolute joint. The finished six-bar is shown in Fig. 3. 2. (c).

5. Check the transmission angles.

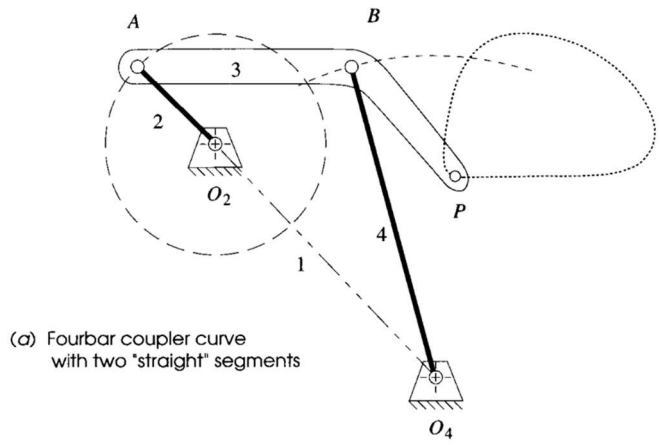


(a) **Fourbar coupler curve with 2 straight-line segments.**

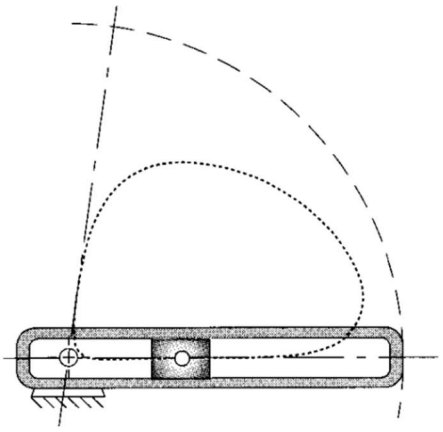

(b) **Slider joint dyad for double dwell.**

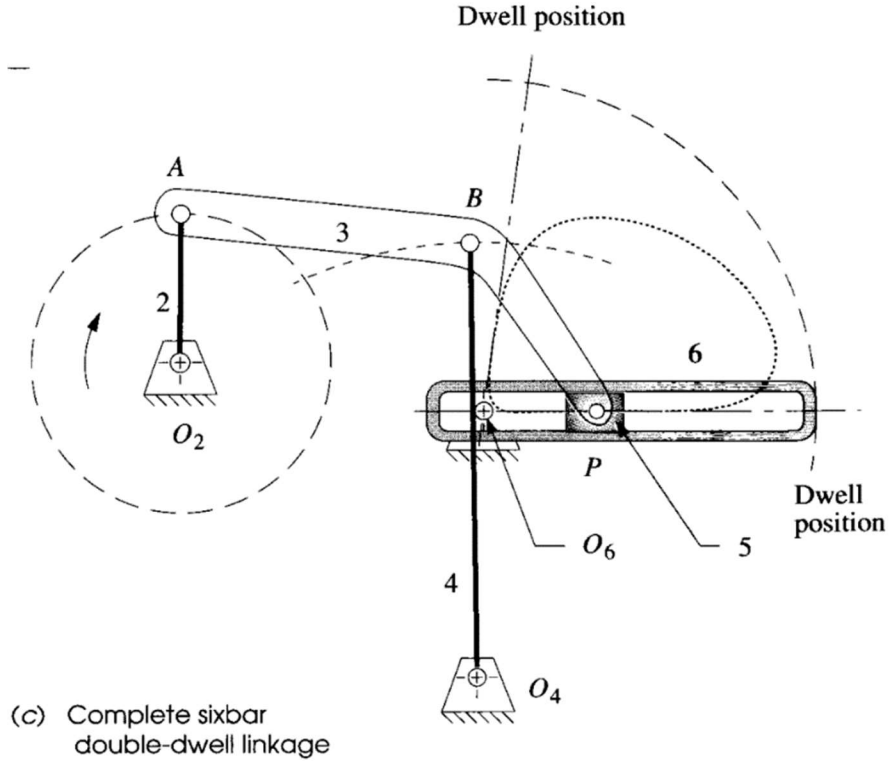


(c) **Complete six-bar double dwell linkage.**

**Fig. 3. 2**: Design process of a complete 6-bar double dwell linkage based on a coupler curve with 2 straight line segments [Nor99, S. 129].

This method is not considered very exhaustive, as there seems to be a considerable space for imprecision in the overlay of two straight lines over the irregular coupler curve (Fig. 3. 2 (b)). The actual output motion is not found likely to dwell for as long or as accurately as in the graphic representation.

#### 3.1.1.3 Single arc dwell design

Another complete design process for a 6-bar double dwell linkage is proposed in *Design of Machinery* [Nor99, S. 126–127]. In this case, it is a single-dwell arc linkage. The following motion properties can be adjusted:

- Rocker-crank motion relationship
- Dwell motion angle in crank cycle

The full design process is explained step by step for a six-bar linkage with a 90º rocker motion over 300 crank degrees with dwell for the remaining 60º.

1. Search the H&N atlas for a four-bar linkage with a coupler curve having an approximate (pseudo) circle arc portion which occupies 60° of crank motion (12 dashes on the atlas). The chosen four-bar is shown in Fig. 3. 3 (a).
2. Layout this linkage to scale including the coupler curve and find the approximate center of the chosen coupler curve pseudo-arc using graphical geometric techniques. To do so, draw the chord of the arc and construct its perpendicular bisector as shown in Fig. 3.3 (b). The center will lie on the bisector. Label this point D.
3. Set your compass to the approximate radius of the coupler arc. This will be the length of link 5 which is to be attached at the coupler point P.
4. Trace the coupler curve with the compass point, while keeping the compass pencil lead on the perpendicular bisector and find the extreme location along the bisector that the compass lead will reach. Label this point E.
5. The line segment DE represents the maximum displacement that a link of length $\overline{CD}$, attached at P, will reach along the bisector.
6. Construct a perpendicular bisector of the line segment $\overline{DE}$ and extend it in a convenient direction.
7. Locate fixed pivot $O_6$ on the bisector of $\overline{DE}$ such that lines $\overline{O_6D}$ and $\overline{O_6E}$ subtend the desired output angle, in this example, 90º.
8. Draw link 6 form D (or E) through $O_6$ and extend to any convenient length. This is the output link which will dwell for the specified portion of the crank cycle.
9. Check the transmission angles.
10. Make a cardboard model of the linkage and articulate it to check its function.

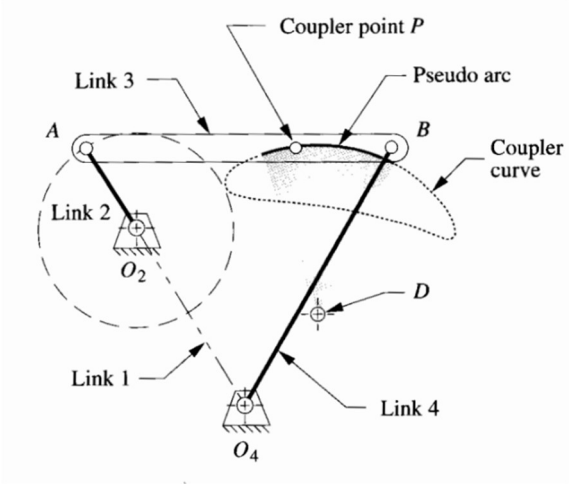


(a) **Chosen four-bar crank-rocker with pseudo-arc section for 60º of link 2 rotation**

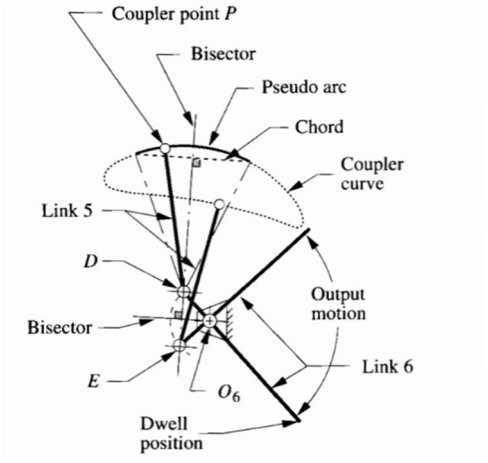


(b) **Construction of the output-dwell dyad**

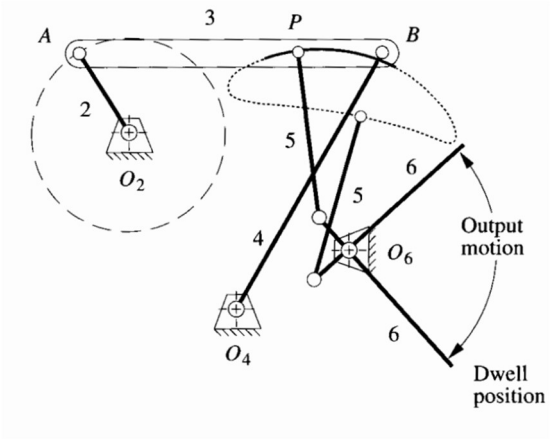


(c) **Completed six-bar single-dwell linkage with rocker output motion**

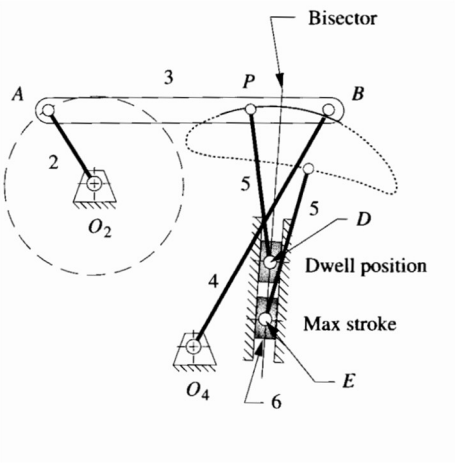


(d) **Completed six-bar single dwell linkage with slider output motion**

**Fig. 3. 3**: Design process of a complete 6-bar single dwell with rocker output or slider output, using on a coupler curve with 1 arc segment [Nor99, S. 127].

Finally, this last method is chosen due its level of detail and the availability of the necessary resources. It is considered that such a linkage can be designed from the start using the H&N Atlas of Coupler Curves. Therefore, a single-dwell 6-bar linkage based on a coupler curve with 1 arc segment will be designed.

# 4 Dwell Linkage Design: Application of the chosen Method

The chosen method will be applied. Its first steps involving the H&N Atlas are shown in Fig. 4. 1:

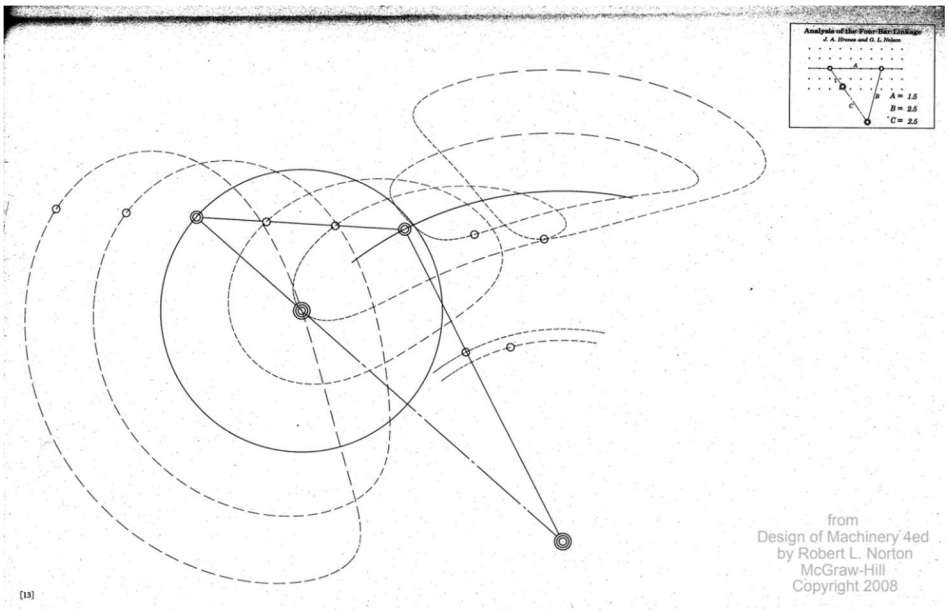


(a) **Chosen page from the H&N Atlas. A suitable coupler curve for the design method must be chosen.**

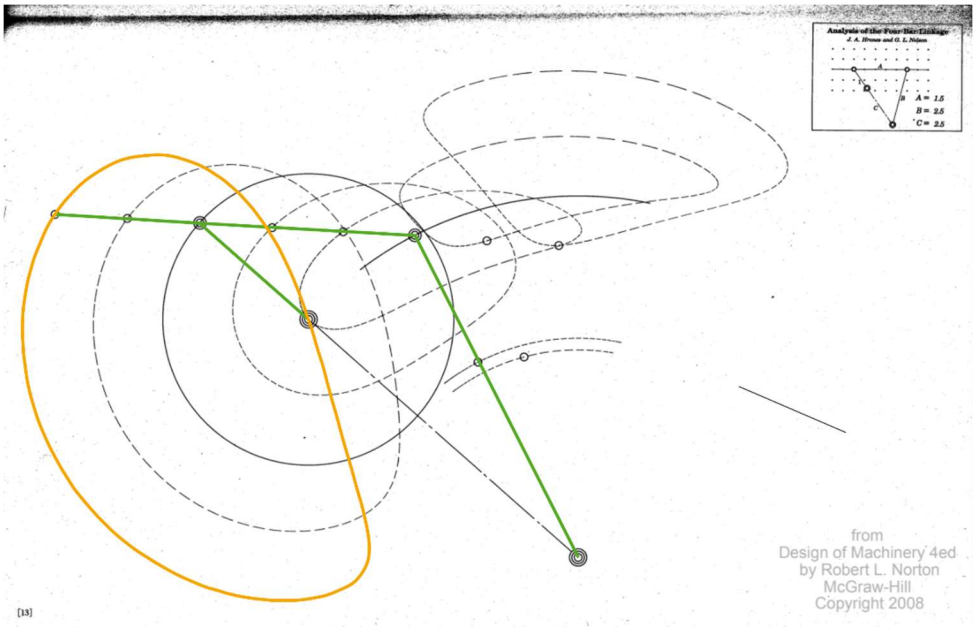


(b) **Identification of the four-bar linkage (on green), and the coupler curve it traces (on yellow). The coupler point on the left end has been chosen due to the prominent circular arc it traces.**

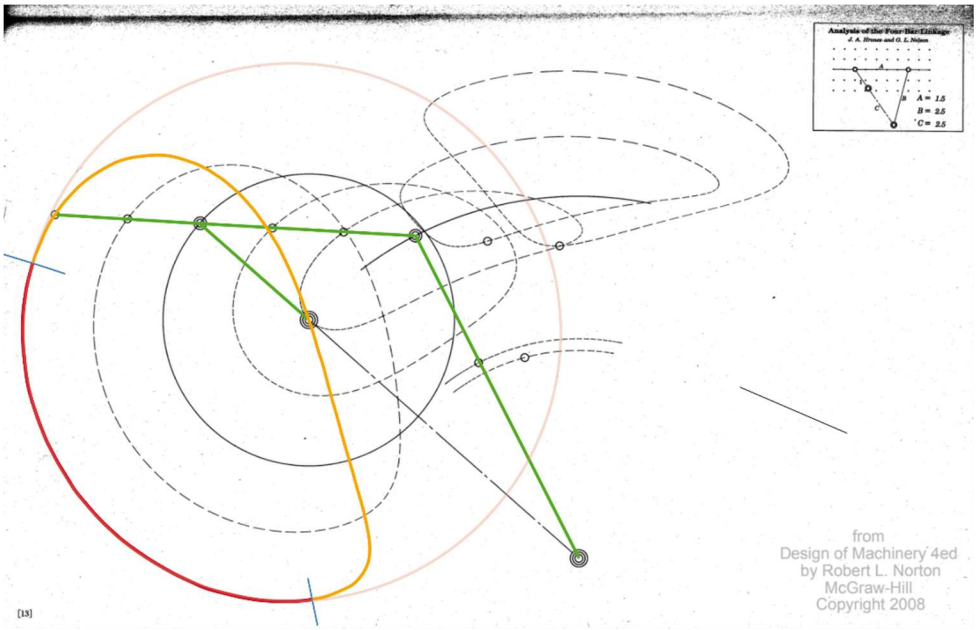


(c) **Identification of the circular coupler curve segment (on red, limited by blue lines at both ends). This segment occupies 28 dashes on the coupler curve, which correspond to 140 degrees in the rotation of the crank.**

**Fig. 4. 1**: Preparation for the single arc dwell graphic method, using the H&N Atlas of Coupler Curves [HN51, S. 13].

Now, the graphic method explained on section 2.4.2.3. can be performed, as shown in the Appendix A. To provide a better visualization of the graphically obtained six-bar linkage dwell mechanism, a virtual representation has been designed.

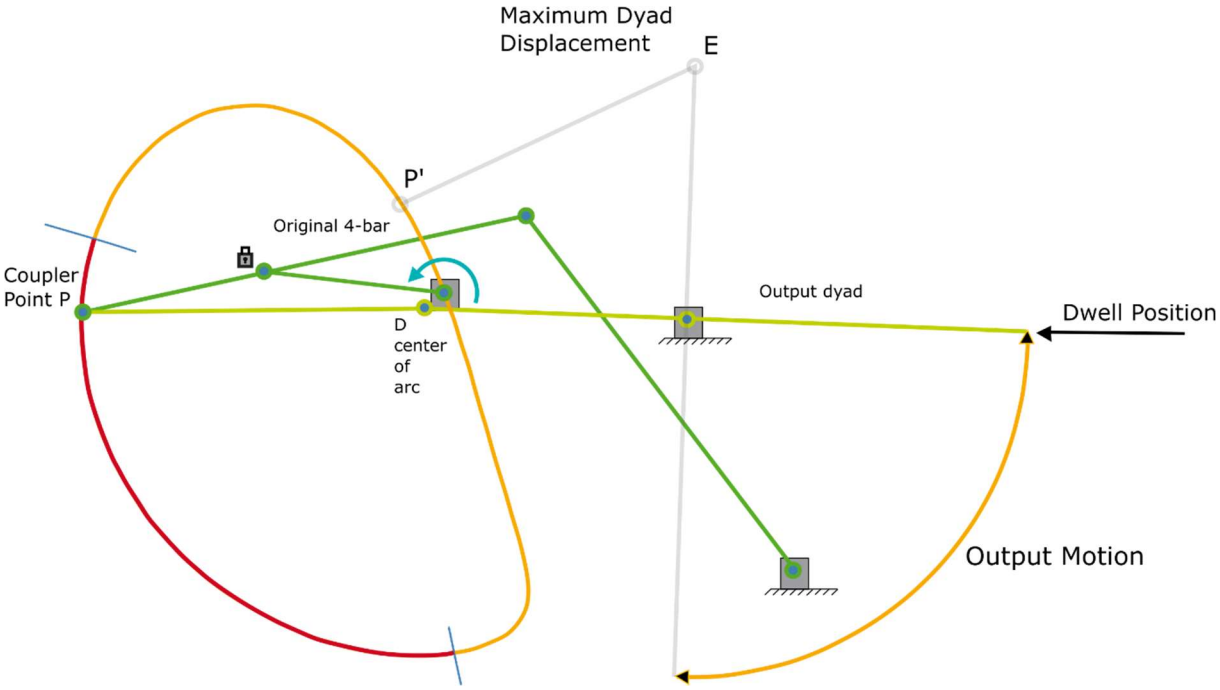


**Fig. 4. 2**: Representation of the result of the graphic method, indicating the original 4-bar linkage, the additional dyad, the circular coupler curve segment, the output motion, and the dwell position.

It has been decided to design an output motion of 90 degrees. Therefore, the fixed pivot of the dyad has been placed on the bisector of DE such its lines with $D$ and $E$ subtend this angle. Therefore, a 6-bar linkage that dwells for 140 degrees of crank rotation and has an output motion of 90 degrees has been designed. In order to study the designed linkage further, it will be simulated using MechDev, as mentioned on section 2.3.1.2. There, its coupler curve and output motion can be estimated again and compared to the graphically obtained ones.

## 4.1 Simulation in MechDev

The results of the simulation on MechDev are shown in Figs. 4. 3 and 4. 4:

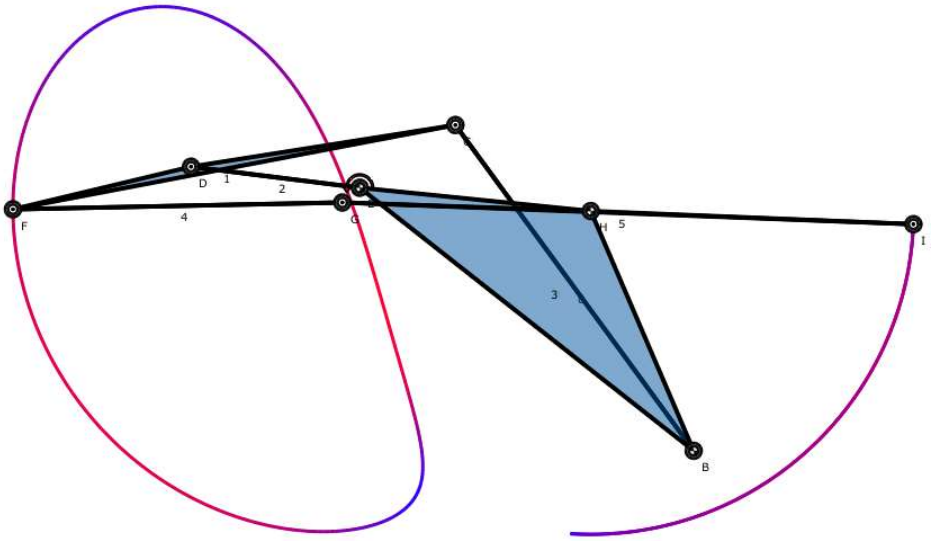


**Fig. 4. 3**: Simulated 6-bar dwell linkage in the same initial position as in Fig. 4. 2.

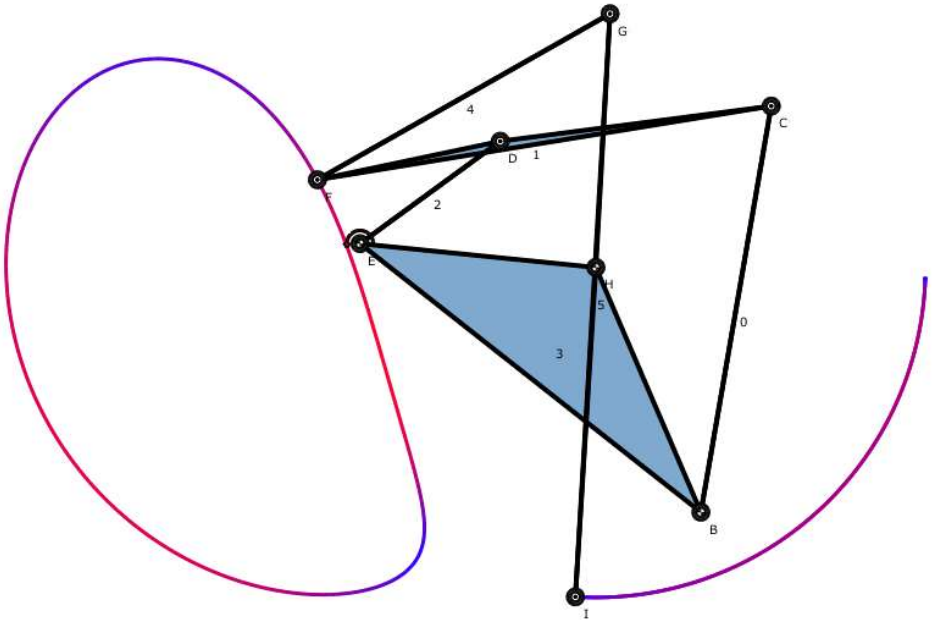


**Fig. 4. 4**: Simulated 6-bar dwell linkage in its "maximum dyad displacement" position (dyad represented on grey in Fig. 4. 2.)

### 4.1.1 Dimensions of the 6-bar linkage

After simulating the linkage on Mechdev, all its dimensions can be determined by studying the joint coordinates (Tab. 4. 1.) and the distances between the joints (Tab. 4. 2.). The input joint $O_2$ is used as a reference.

**Tab. 4. 1:** Coordinates of the fixed joints, in reference to the input joint $\boldsymbol{O_2}$

| Joint | X coordinate (mm) | Y coordinate (mm) |
|---|---|---|
| $\boldsymbol{O_2}$ | 0 | 0 |
| $\boldsymbol{O_4}$ | 1060,14 | -834,20 |
| $\boldsymbol{O_6}$ | 733,47 | -73,88 |

**Tab. 4. 2:** Link lengths. For links 3 and 6, their sub-link distances are shown.

| Link | Dimension/Sub-dimensions | Joints | Length (mm) |
|---|---|---|---|
| 2 | $L_2$ | $O_2 - A$ | 539,95 |
| 3 | $L_{3,1}$ | $A - B$ | 849,83 |
| | $L_{3,2}$ | $A - C$ | 581,33 |
| 5 | $L_5$ | $C - D$ | 1046,09 |
| 6 | $L_{6,1}$ | $D - O_6$ | 789,30 |
| | $L_{6,2}$ | $O_6 - E$ | 789,30 |
| 4 | $L_4$ | $B - O_4$ | 1280,47 |
| 1 | $L_1$ | $O_2 - O_4$ | 1348,99 |

### 4.1.2 Coupler Link

It is shown in Fig. 4.3 and Fig. 4.4. that the coupler curve is not a straight line with three joints, but it has a triangular shape, albeit with a small height in proportion to its base dimension. This happens because the position of the joint between the crank and the coupler link has been slightly modified so that the coupler curve fits the graphically obtained coupler curve better, especially in its arc segment. Therefore, it must be taken into account how dimensions $L_{3,1}$ and $L_{3,2}$ in the coupler link have different angles:

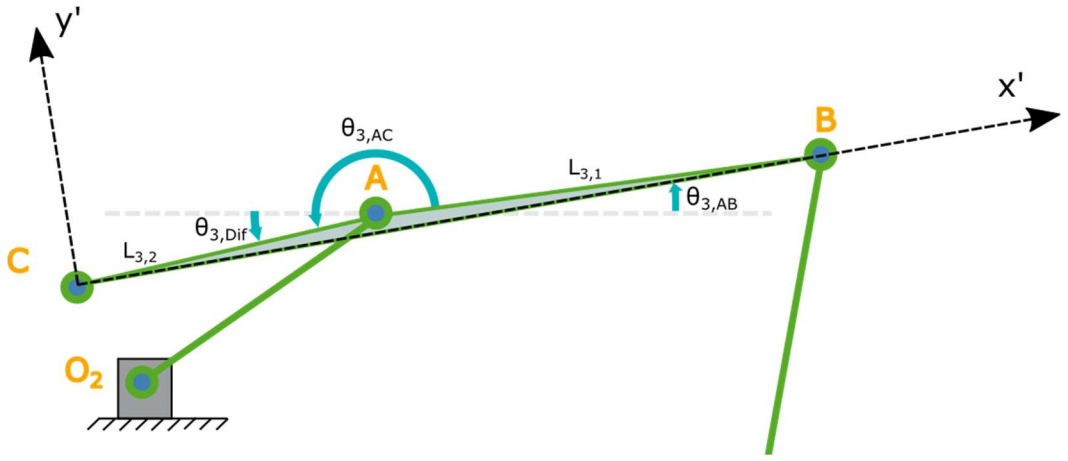


**Fig. 4. 5**: Representation of the coupler link designed in MechDev, as shown in Fig. 4.3 and Fig. 4.4. Slight differences in the angles of its different dimensions are taken into account.

The exact angles have been obtained using the joint coordinates provided by MechDev and are shown in Tab. 4. 3.:

**Tab. 4. 3:** Coupler link angles.

| Symbol | Angle (°) |
|---|---|
| $\theta_{3,AC}$ | 193,44 |
| $\theta_{3,AB}$ | 8,95 |
| $\theta_{3,Dif}$ | 4,49 |

The dimensions of this triangular link can be obtained with these angles and distances $L_{3,1}$ and $L_{3,2}$. They can be expressed using relative coordinate axes in the coupler link (x' and y' in Fig. 4. 5.), parallel to the base and height of the triangle:

**Tab. 4. 4:** Coupler link dimensions.

| Symbol | Coupler Link Dimensions (mm) |
|---|---|
| $R_{CA,x'}$ | 565,42 |
| $R_{AB,x'}$ | 839,48 |
| $R_{CB,x'}$ | 1404,90 |
| $R_{CB,y'}$ | 135,07 |

Dimensions $R_{CB,x'}$ and $R_{CB,y'}$ correspond to the base and height dimensions of the triangular link.

# 5 Energy Efficiency Study: Application of Eigenmotion for the designed Dwell Mechanism

In order to calculate the Eigenmotion of the mechanism, it must be formulated in a way that includes the mechanism properties. It will be set following equations from [SHC17].

Firstly, the kinetic energy has to be set up. The kinetic energy of the mechanism can be written as the sum of the kinetic energy of its six links:

$$E_{kin} = \sum_{i=1}^{6} E_{kin,i} \tag{5.1}$$

The kinetic energy of a rigid body can be split into a translational (T) and a rotational (R) part:

$$E_{kin,i} = E_{kin,Ti} + E_{kin,Ri} = \left(\frac{1}{2} \cdot \sum_{i=1}^{n} m_i \cdot {v_{CM,i}}^2\right) + \left(\frac{1}{2} \cdot \sum_{i=1}^{n} J_i \cdot {\dot{\theta}_i}^2\right) \tag{5.2}$$

where $v_{CM,i}$ refers to the center mass speed for the link $i = 1,2, \dots, 6$ :

$${v_{CM,i}}^2 = \left[\frac{dx_{CM,i}}{dt}\right]^2 + \left[\frac{dy_{CM,i}}{dt}\right]^2 \tag{5.3}$$

And $J_i$ refers to the mass moment of inertia for the link *i*. For straight links that rotate about an end, it can be expressed as:

$$J_{i,ER} = \frac{1}{3} \cdot m_i \cdot {L_i}^2 \tag{5.4}$$

For straight links that rotate around their center, it can be expressed as:

$$J_{i,CR} = \frac{1}{12} \cdot m_i \cdot {L_i}^2 \tag{5.5}$$

In the case links rotate about a point at a distance $d$ from an end, Steiner's theorem can be applied.

$$J_i = \frac{1}{3} \cdot m_i \cdot {L_i}^2 + m_i \cdot d^2 \tag{5.6}$$

And $\dot{\theta}_i$ refers to the angular speed for each link:

$$\dot{\theta}_i = \frac{d\theta_i}{dt} \tag{5.7}$$

Using Equations 6.2. and. 6.3., The kinetic energy of the crank can be written as:

$$E_{kin,2} = E_{kin,T2} + E_{kin,R2} = \frac{1}{2} m_2 \left( \left[ \frac{dx_{CM,2}}{dt} \right]^2 + \left[ \frac{dy_{CM,2}}{dt} \right]^2 \right) + \frac{1}{2} J_2 \, \dot{\varphi}^2 \tag{5.8}$$

$$= \frac{1}{2} m_2 \left( \left[ \frac{dx_{CM,2}}{d\varphi} \right]^2 + \left[ \frac{dy_{CM,2}}{d\varphi} \right]^2 \right) \dot{\varphi}^2 + \frac{1}{2} J_2 \, \dot{\varphi}^2 \tag{5.9}$$

$$= \left( \frac{1}{2} m_2 \left( \left[ \frac{dx_{CM,2}}{d\varphi} \right]^2 + \left[ \frac{dy_{CM,2}}{d\varphi} \right]^2 \right) + \frac{1}{2} J_2 \right) \dot{\varphi}^2 \tag{5.10}$$

$$= \frac{1}{2} J_{red,2}(\varphi) \, \dot{\varphi}^2 \tag{5.11}$$

The kinetic energy of link 1 is zero, because it is the fixed linked and there is no rotation or translation in it. That is, $E_{kin,1} = 0$.

For the remaining links, $(i = 3, \dots, 6)$, the kinetic energy can be written as:

$$E_{kin,i} = E_{kin,Ti} + E_{kin,Ri} = \frac{1}{2} m_i \left( \left[ \frac{dx_{CM,i}}{dt} \right]^2 + \left[ \frac{dy_{CM,i}}{dt} \right]^2 \right) + \frac{1}{2} J_i \, \dot{\varphi}^2 = \tag{5.12}$$

$$= \left( \frac{1}{2} m_i \left( \left[ \frac{dx_{CM,i}}{d\varphi} \right]^2 + \left[ \frac{dy_{CM,i}}{d\varphi} \right]^2 \right) + \frac{1}{2} J_i \right) \dot{\varphi}^2 = \tag{5.13}$$

$$= \frac{1}{2} J_{red,i}(\varphi) \, \dot{\varphi}^2 \tag{5.14}$$

$$E_{kin,i} = E_{kin,Ti} + E_{kin,Ri} = \frac{1}{2} m_i \left( \left[ \frac{dx_{CM,i}}{dt} \right]^2 + \left[ \frac{dy_{CM,i}}{dt} \right]^2 \right) + \frac{1}{2} J_i \, \dot{\varphi}^2 =$$

$$= \left( \frac{1}{2} m_i \left( \left[ \frac{dx_{CM,i}}{d\varphi} \right]^2 + \left[ \frac{dy_{CM,i}}{d\varphi} \right]^2 \right) + \frac{1}{2} J_i \right) \dot{\varphi}^2 =$$

$$= \frac{1}{2} J_{red,i}(\varphi) \, \dot{\varphi}^2 \tag{5.15}$$

Therefore:

$$E_{kin} = \sum_{i=1}^{6} E_{kin,i} = \sum_{i=1}^{6} \frac{1}{2} J_{red,i}(\varphi) \, \dot{\varphi}^2 = \frac{1}{2} J_{red}(\varphi) \, \dot{\varphi}^2 \tag{5.16}$$

for:

$$J_{red}(\varphi) = \sum_{i=1}^{6} J_{red,i}(\varphi) \tag{5.17}$$

The Eigenmotion of a mechanism is defined as its intrinsic motion in the case of constant kinetic energy. It is denoted by the index 'e':

$$E_{kin} = \frac{1}{2} J_{red}(\varphi)\, \dot{\varphi_e}^2 = const. = \frac{1}{2} J_{red}(\varphi_0)\, \dot{\varphi_0}^2 \tag{5.18}$$

The Eigenmotion is obtained from:

$$\dot{\varphi_e} = \frac{\dot{\varphi_0}\sqrt{J_{red}(\varphi_0)}}{\sqrt{J_{red}(\varphi)}} = \frac{C}{\sqrt{J_{red}(\varphi)}} \tag{5.19}$$

The numerator of the equation is constant and denoted by C. In order to obtain $J_{red}(\varphi)$, the mass center position of the links and their mass moment of inertia as a function of the crank angle $\varphi$ must be obtained. Therefore, a kinematic analysis of the 6-bar linkage will now be performed.

## 5.1 Kinematic Analysis of the Dwell Mechanism

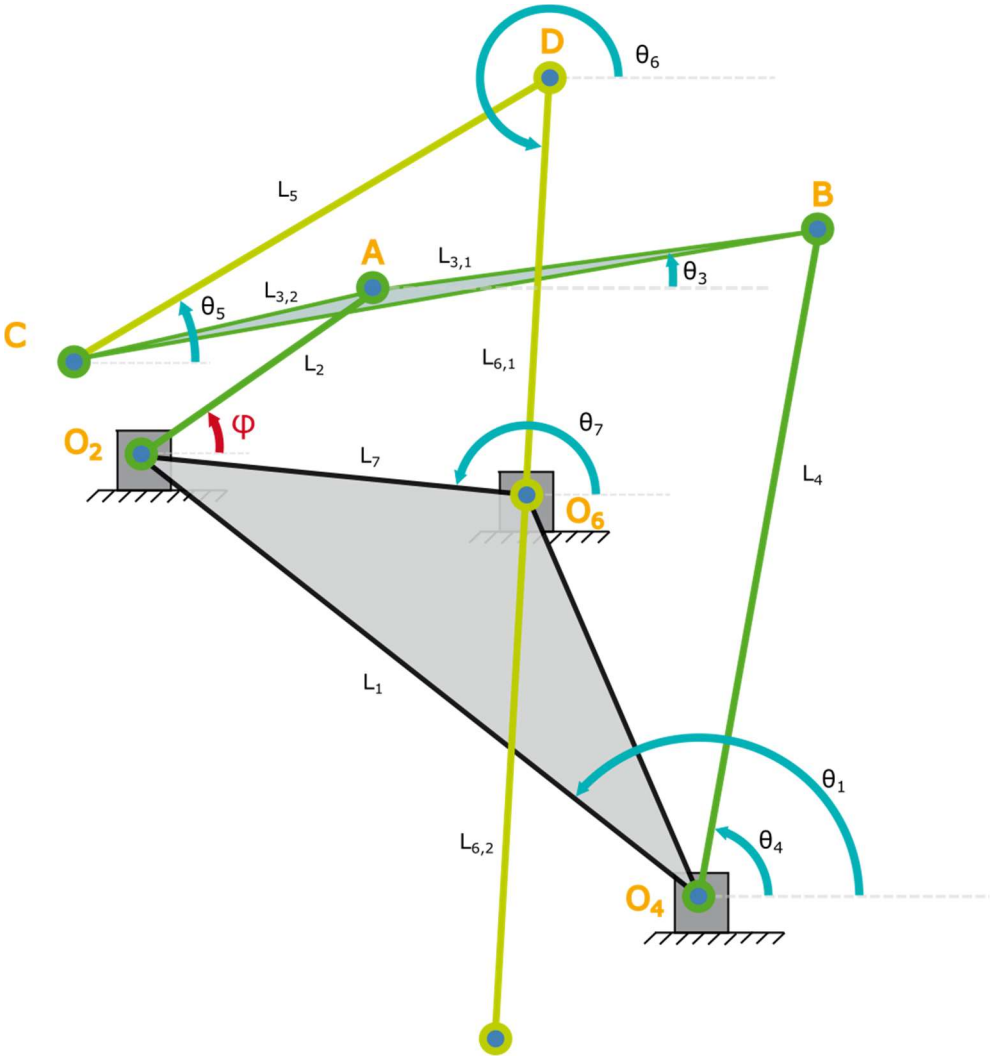


**Fig. 5. 1**: Representation of the full 6-bar linkage in its "maximum dyad displacement" position with its joint names, link angles and link dimensions.

In order to perform the kinematic analysis, the loop closure equation (or vector loop equation) will be applied [UPS17, S. 57–61]. The six-bar linkage will be divided into 2 interconnected closed sub-chains:

1. A 4-bar sub-chain: The 4-bar taken from the original H&N Atlas (depicted in dark green on Fig. 5. 1), including links 1, 2, 3, 4.

2. A dyad sub-chain: five-bar linkage, including links 1, 2, 3, 5, 6.

### 5.1.1 4-bar sub-chain

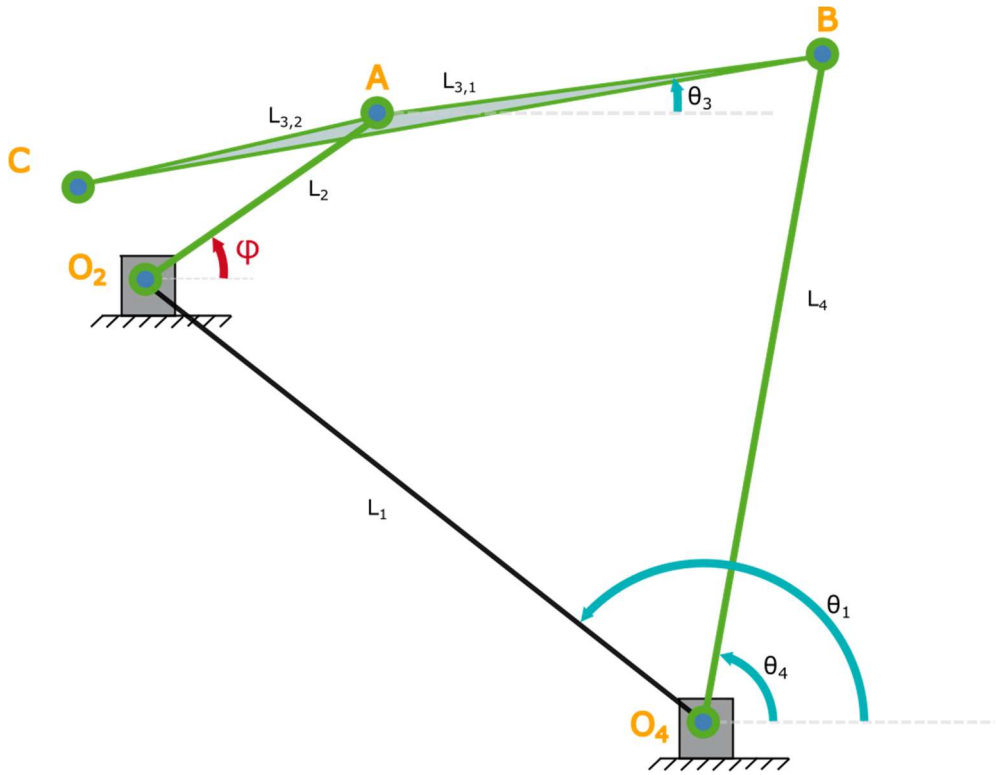


**Fig. 5. 2**: Representation of the 4-bar sub-chain its link angles and dimensions.

The vector loop equation for the four-bar sub-chain would be:

$$\boldsymbol{r}_{O_2A} + \boldsymbol{r}_{AB} - \boldsymbol{r}_{O_4B} - \boldsymbol{r}_{O_2O_4} = 0 \tag{5.20}$$

#### 5.1.1.1 Position Equations

Developing the vector loop equation with the link lengths and angles expressed on Fig. 5.2., the position equations for the 4-bar sub-chain are obtained for the horizontal and vertical axes:

$$L_2 \cos(\varphi) + L_{3,1} \cos(\theta_3) - L_4 \cos(\theta_4) - L_1 \cos(\theta_1) = 0 \tag{5.21}$$

$$L_2 \sin(\varphi) + L_{3,1} \sin(\theta_3) - L_4 \sin(\theta_4) - L_1 \sin(\theta_1) = 0 \tag{5.22}$$

These equations will be solved numerically to obtain $\theta_3$ and $\theta_4$ as a function of crank angle $\varphi$.

#### 5.1.1.2 Speed Equations

The speed equations are obtained through the derivation of eq. (5. 21) and eq. (5. 22):

$$-L_2 \sin(\varphi)(\dot{\varphi}) - L_{3,1} \sin(\theta_3)(\dot{\theta}_3) + L_4 \sin(\theta_4)(\dot{\theta}_4) + L_1 \sin(\theta_1)(\dot{\theta}_1) = 0 \quad \textbf{(5.23)}$$

$$L_2 \cos(\varphi)(\dot{\varphi}) + L_{3,1} \cos(\theta_3)(\dot{\theta}_3) - L_4 \cos(\theta_4)(\dot{\theta}_4) - L_1 \cos(\theta_1)(\dot{\theta}_1) = 0 \quad \textbf{(5.24)}$$

### 5.1.2 Dyad sub-chain

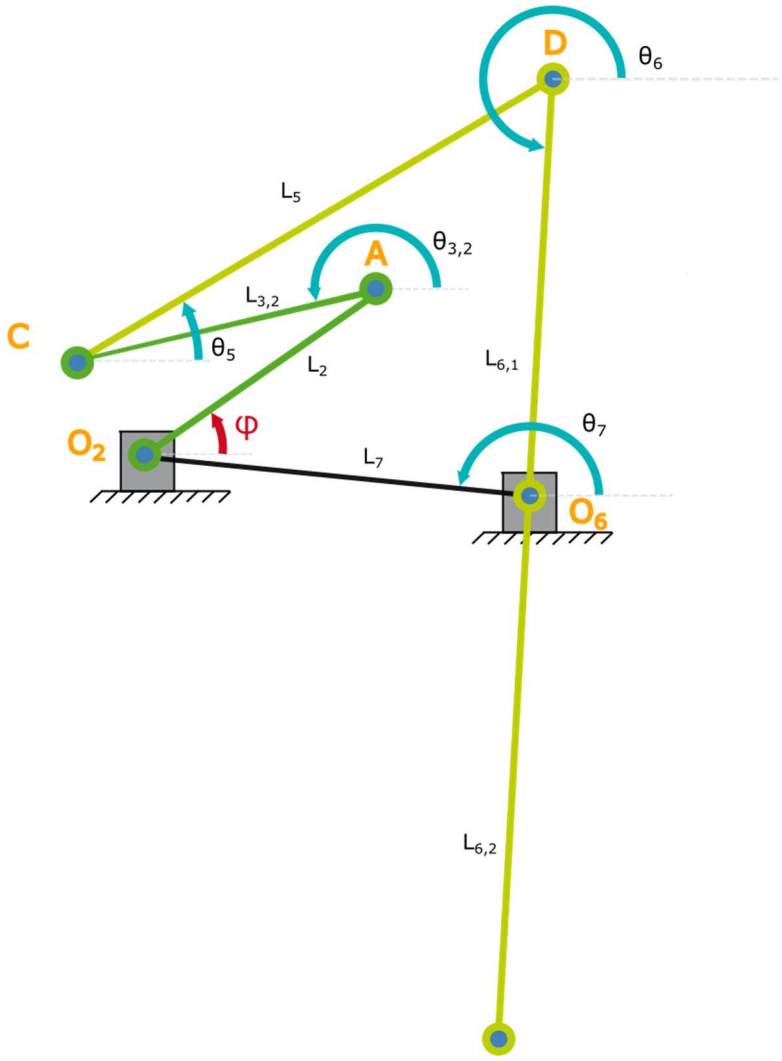


**Fig. 5. 3**: Representation of the dyad sub-chain, with its link angles and dimensions.

The vector loop equation for the dyad sub-chain would be:

$$\boldsymbol{r}_{O_2A} + \boldsymbol{r}_{AC} - \boldsymbol{r}_{DC} - \boldsymbol{r}_{O_6D} - \boldsymbol{r}_{O_2O_6} = 0 \quad \textbf{(5.25)}$$

#### 5.1.2.1 Position Equations

Developing the vector loop equation with the link lengths and angles expressed on Fig. 5.3., the position equations for the 4-bar sub-chain are obtained for the horizontal and vertical axes:

$$L_2\cos(\varphi) + L_{3,2}\cos(\theta_3 - 180) - L_7\cos(\theta_7 + 180) - L_{6,1}\cos(\theta_6 + 180) - L_5\cos(\theta_5) = 0 \quad \textbf{(5.26)}$$

$$L_2\sin(\varphi) + L_{3,2}\sin(\theta_3 - 180) - L_7\sin(\theta_7 + 180) - L_{6,1}\sin(\theta_6 + 180) - L_5\sin(\theta_5) = 0 \quad \textbf{(5.27)}$$

These equations will be solved numerically to obtain $\theta_5$ and $\theta_6$ as a function of crank angle $\varphi$. Angle $\theta_3$ is obtained from the position equations of the 4-bar sub-chain and $\theta_7$ is constant.

#### 5.1.2.2 Speed Equations

The speed equations are obtained through the derivation of the position equations:

$$-L_2\sin(\varphi)(\dot{\varphi}) - L_{3,2}\sin(\theta_3 - 180)(\dot{\theta_3}) + L_7\sin(\theta_7 + 180)(\dot{\theta_7}) + L_{6,1}\sin(\theta_6 + 180)(\dot{\theta_6}) + L_5\sin(\theta_5)(\dot{\theta_5}) = 0 \quad \textbf{(5.28)}$$

$$L_2\cos(\varphi)(\dot{\varphi}) + L_{3,2}\cos(\theta_3 - 180)(\dot{\theta_3}) - L_7\cos(\theta_7 + 180)(\dot{\theta_7}) - L_{6,1}\cos(\theta_6 + 180)(\dot{\theta_6}) - L_5\cos(\theta_5)(\dot{\theta_5}) = 0 \quad \textbf{(5.29)}$$

### 5.1.3 Mass Center Position Equations

- Link 2

$$x_{CM,2} = \frac{L_2}{2}\cos(\varphi) \quad \textbf{(5.30)}$$

$$y_{CM,2} = \frac{L_2}{2}\,\text{sen}(\varphi) \quad \textbf{(5.31)}$$

- Link 4

$$x_{CM,4} = x_{O_4} + \frac{L_4}{2}\cos(\theta_4) \quad \textbf{(5.32)}$$

$$y_{CM,4} = y_{O_4} + \frac{L_4}{2}\sin(\theta_4) \quad \textbf{(5.33)}$$

- Link 3

$$x_{CM,3} = x_{O_4} + L_4 \cos(\theta_4) - \frac{(L_{3,1} + L_{3,2})}{2} \cos(\theta_3) \quad \textbf{(5.34)}$$

$$y_{CM,3} = y_{O_4} + L_4 \sin(\theta_4) - \frac{(L_{3,1} + L_{3,2})}{2} \sin(\theta_3) \quad \textbf{(5.35)}$$

- Link 5

$$x_{CM,5} = x_{O_6} + \frac{L_6}{2} \cos(\theta_6 + 180) + \frac{L_5}{2} \cos(\theta_5) \quad \textbf{(5.36)}$$

$$y_{CM,5} = y_{O_6} + \frac{L_6}{2} \sin(\theta_6 + 180) + \frac{L_5}{2} \sin(\theta_5) \quad \textbf{(5.37)}$$

- Link 6: Because $L_{6,1} = L_{6,2}$:

$$x_{CM,6} = x_{O_6} \quad \textbf{(5.38)}$$

$$y_{CM,6} = y_{O_6} \quad \textbf{(5.39)}$$

### 5.1.4 Mass Moment of Inertia Equations

In order to express the mass moments of inertia for each link $(J_i)$, coherent mass values must be assigned to each link in the mechanism. The following assumptions will be made:

- Each link is a straight rod with a section of 1 $cm^2$ and its specific length.
- The coupler link of the mechanism (link 3), despite having a triangular shape, will be simplified as a straight link due to its small height dimension in comparison to its base dimension in the triangle.
  - Base dimension: $R_{CB,x} = 1404{,}9\ mm$
  - Height dimension: $R_{CB,y} = 135{,}07438\ mm$

  This assumption simplifies the calculation of its mass moment of inertia.

- All the links have the density of aluminum, which can be expressed as a linear density:

$$\rho = \rho_{Al} = 2{,}7\ {}^{g}/_{cm^3} = 0{,}27\ {}^{kg}/_{(cm^2 \cdot m)} \quad \textbf{(5.40)}$$

**Tab. 5. 1:** Link dimensions, lengths, and masses for a 1 $\boldsymbol{cm^2}$ section.

| Link | Dimension/Sub-dimensions | Length (mm) | Mass (g) |
|---|---|---|---|
| 2 | $L_2$ | 539,95 | 146,33 |
| 3 | $L_{3,1}$ | 849,83 | 230,30 |
| | $L_{3,2}$ | 581,33 | 157,54 |
| 5 | $L_5$ | 1046,09 | 283,49 |
| 6 | $L_{6,1}$ | 789,30 | 213,90 |
| | $L_{6,2}$ | 789,30 | 213,90 |
| 4 | $L_4$ | 1280,47 | 347,02 |
| 1 | $L_1$ | 1348,99 | 365,58 |

- Link 2: The crank rotates around joint $O_2$ at its end:

$$J_2 = \frac{1}{3} \cdot m_2 \cdot {L_2}^2 \tag{5.41}$$

- Link 3: Steiner's theorem is applied, considering link 3 as a straight link that rotates around joint A, which doesn't coincide with its middle point:

$$J_3 = \frac{1}{12} \cdot m_3 \cdot \left(L_{3,1} + L_{3,2}\right)^2 + m_3 \cdot \left(\left(x_A - \frac{(x_B + x_C)}{2}\right)^2 + \left(y_A - \frac{(y_B + y_C)}{2}\right)^2\right) \tag{5.42}$$

- Link 4: Rotates (partly) around joint $O_4$ at its end:

$$J_4 = \frac{1}{3} \cdot m_4 \cdot {L_4}^2 \tag{5.43}$$

- Link 5: Rotates around joint $C$ at its end:

$$J_5 = \frac{1}{3} \cdot m_5 \cdot {L_5}^2 \tag{5.44}$$

- Link 6: Link 6 rotates around joint $O_6$ at its middle:

$$J_2 = \frac{1}{12} \cdot m_6 \cdot \left(L_{6,1} + L_{6,2}\right)^2 \tag{5.45}$$

## 5.2 Computational calculation of Eigenmotion for the Dwell Mechanism using MATLAB

Now, the behaviour of the six-bar dwell linkage will be studied before and after the application of Eigenmotion, using MatLab. Its process steps can be described as shown in Fig. 5.4:

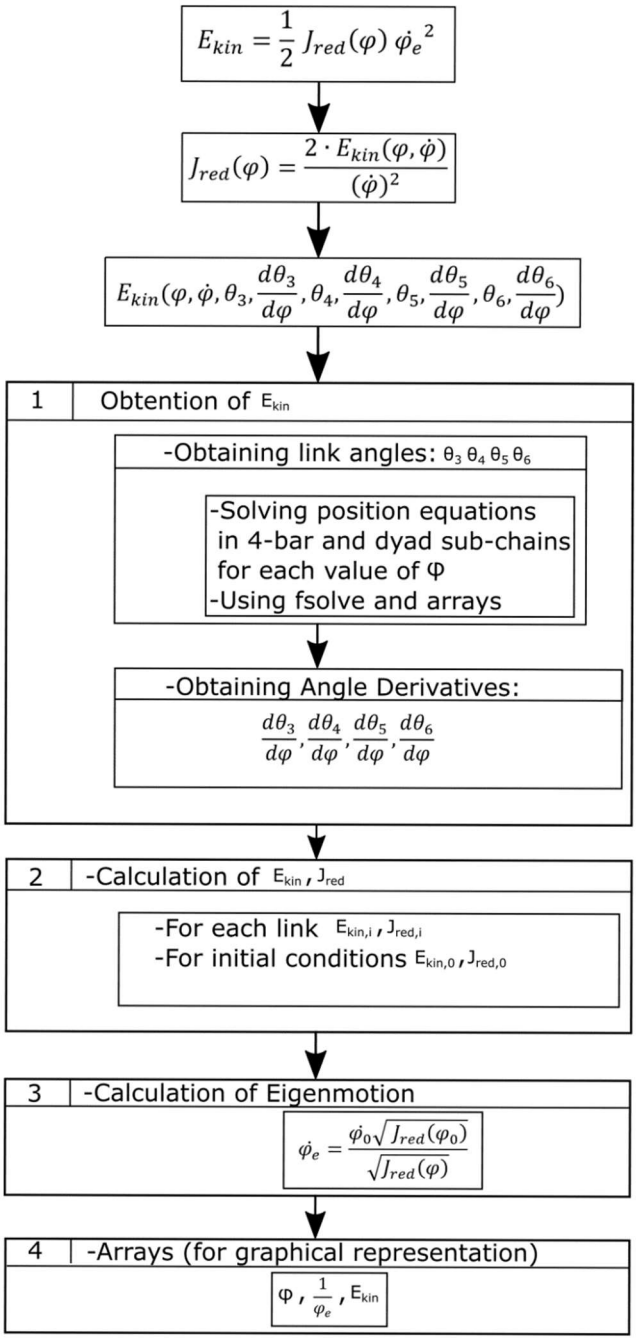


**Fig. 5. 4**: Conceptual representation of the MATLAB computation process.

Firstly, the evolution of the angles $\theta_3$, $\theta_4$, $\theta_5$, $\theta_6$ in the six-bar linkage can be graphically represented for a full cycle, as shown in Fig. 5.5.

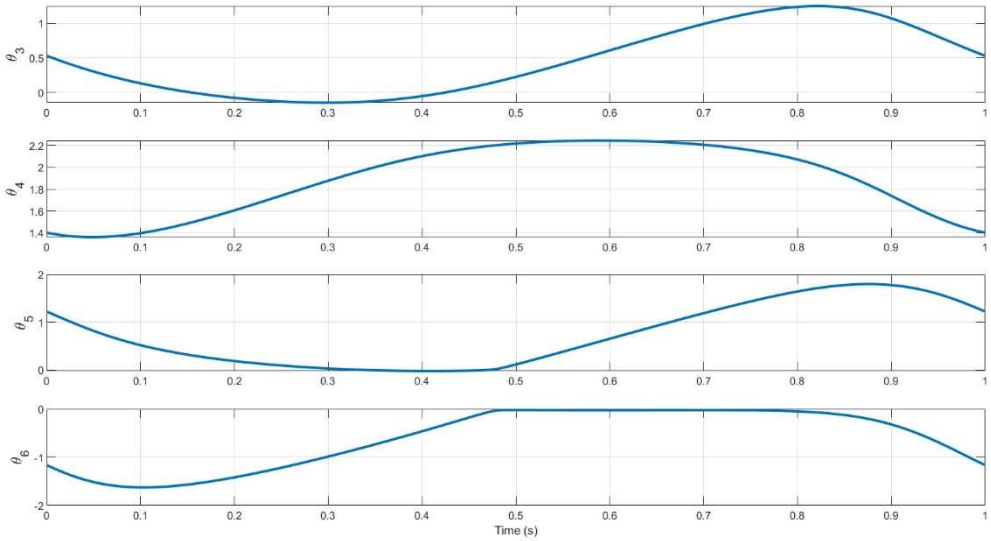


**Fig. 5. 5:** Representation of the link angles $\boldsymbol{\theta_3}$, $\boldsymbol{\theta_4}$, $\boldsymbol{\theta_5}$, $\boldsymbol{\theta_6}$ along a full crank cycle, for a crank speed of $\dot{\boldsymbol{\theta}}_{\boldsymbol{2}} = \boldsymbol{2\pi}\ {}^{\boldsymbol{rad}}/_{\boldsymbol{s}}$. The dwell can be seen on the $\boldsymbol{\theta_6}$ curve (output angle) in the $[\boldsymbol{0, 48 - 0, 8}]\ \boldsymbol{s}$ interval.

The angle derivatives have also been obtained in MATLAB and can be represented in similar conditions, as shown in Fig. 5. 6.

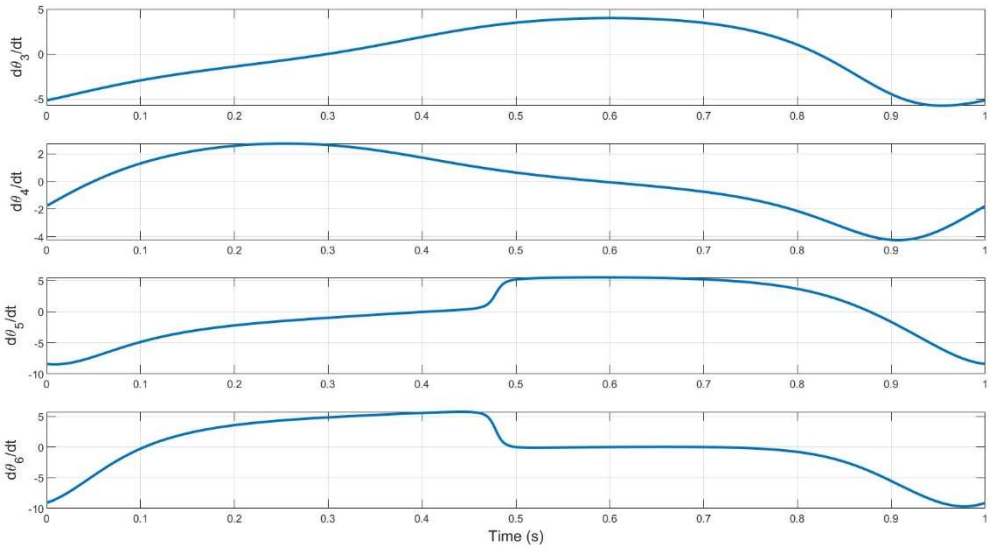


**Fig. 5. 6**: Representation of the link angular speeds $\dot{\boldsymbol{\theta}}_{\boldsymbol{3}}$, $\dot{\boldsymbol{\theta}}_{\boldsymbol{4}}$, $\dot{\boldsymbol{\theta}}_{\boldsymbol{5}}$, $\dot{\boldsymbol{\theta}}_{\boldsymbol{6}}$ along a full crank cycle, for a crank speed of $\dot{\boldsymbol{\theta}}_{\boldsymbol{2}} = \boldsymbol{2\pi}\ {}^{\boldsymbol{rad}}/_{\boldsymbol{s}}$ .

In order to visualize the crank speed evolution before and after operating in Eigenmotion, the crank angles $\varphi$ and $\varphi_e$ are represented along a full cycle, as shown in Fig. 5. 7. The non-constant geometry of the curve $\varphi_e$ corresponds to the varying input speed in Eigenmotion.

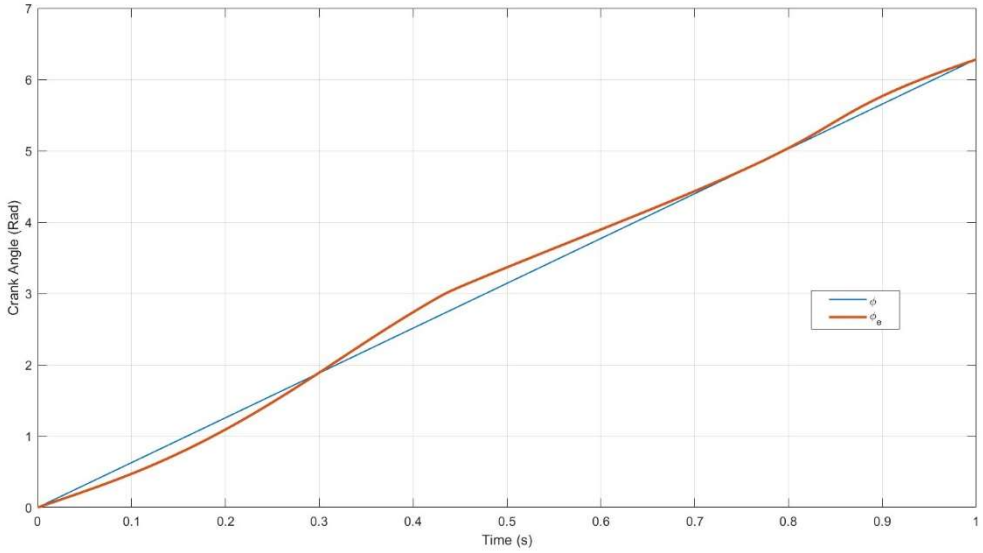


**Fig. 5. 7**: Representation of the angular crank angle in a normal state ($\boldsymbol{\varphi}$, in blue) and in Eigenmotion ($\boldsymbol{\varphi_e}$, in red).

Finally, the output motion (interpreted through the variation of the output angle $\theta_6$) of the dwell mechanism must be visualized before and after the application of Eigenmotion, as shown in Fig. 5. 8.. Increasing the energy efficiency of the mechanism is not the end of the Eigenmotion procedure, since the desired output motion for the mechanism needs to be maintained. Otherwise, whether the application is useful or not depends on the specific requirements; because the exact desired motion cannot be performed anymore by the mechanism.

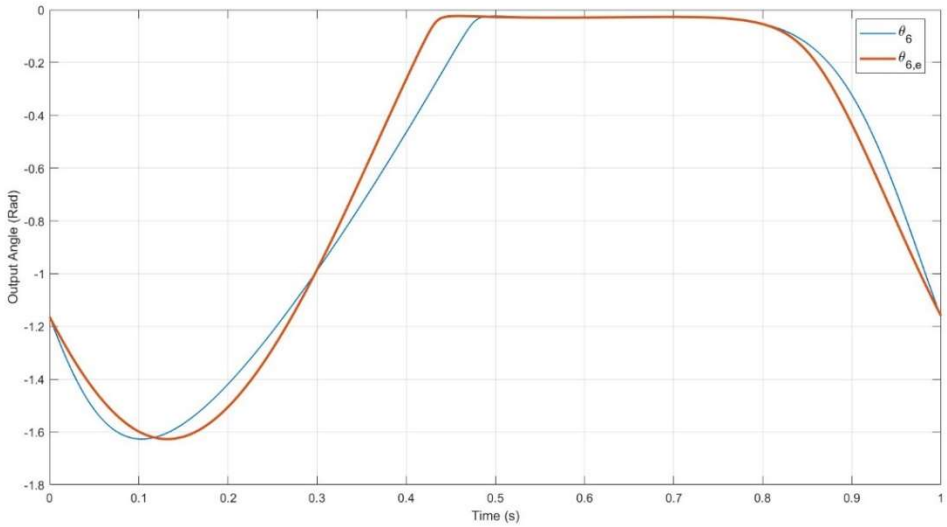


**Fig. 5. 8**: Representation of the output angle in a normal state ($\boldsymbol{\theta_6}$) (in blue) and in Eigenmotion ($\boldsymbol{\theta_{6,e}}$) (in red). An offset between the two motions can be seen.

Even though both motions perform a dwell, Fig. 5. 8 shows an offset between $\theta_{6,e}$ and $\theta_6$, which would mean that the mechanism will not be able to perform the exact same motion while operating in Eigenmotion. Therefore, the obtained output motion in Fig. 5. 8 is not desired as a final result. The following sections address the additional measures that must be implemented to determine if the output motion in Eigenmotion can fit the original motion more accurately.

# 6 Study of possible output motion improvements for the efficient Dwell Mechanism

Previous research has established that the synthesis of mechanisms that perform the originally desired motion while functioning in Eigenmotion is formulated as an optimization problem, minimizing the difference between the resulting output motion (in red in Fig. 5. 8) and the desired motion (in blue in Fig. 5. 8.). It is common to solve this optimization problem using Genetic Algorithms (GA) [SC18; Sch19; SHC17; SHC18].

The overall aim of this post-Eigenmotion section is to adjust the kinematic parameters of the mechanism such that the output motion fits the desired motion [SHC18, S. 405]. Several dimensional parameters will be changed, and the output motion results will be obtained again for dimensional variations until a fitting motion is obtained. The variation corresponding to this last motion will be chosen as the adjusted parameter of the mechanism.

## 6.1 L1 Dimension Adjustment

The resulting output motion (for the mechanism operating in Eigenmotion) is obtained for several variations in the dimension $L_1$, that is, the distance between $O_2$ and $O_4$, the fixed joints of the crank and rocker links of the mechanism. The different variations are:

- $L_1 - 15\ mm$
- $L_1 + 15\ mm$
- $L_1 + 25\ mm$

The output motions of the mechanism with its $L_1$ dimension unchanged is also shown along with the original output motion of the mechanism before Eigenmotion (Fig. 6. 1).

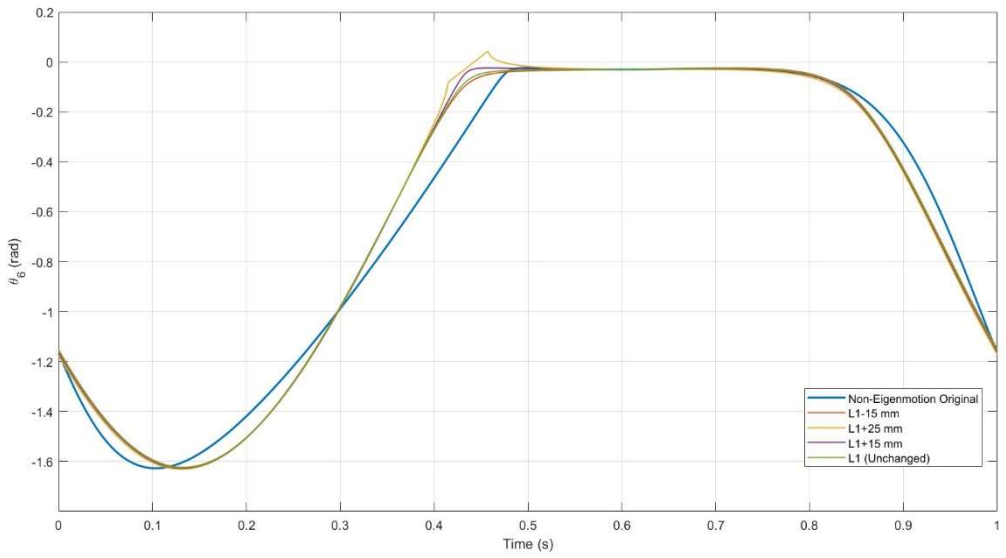


**Fig. 6. 1**: Output motions of the mechanism for different variations of the dimensional parameter $\boldsymbol{L_1}$, along with those of the mechanism with its original dimensions before and after the application of Eigenmotion.

These variations on $L_1$ result in slight variations around the original output motion in Eigenmotion (green in Fig. 6. 1). However, none of these variants fit the original motion (blue) more accurately. Therefore, adjusting $L_1$ on its own is not regarded as a viable method to improve the output motion.

## 6.2 L2 Dimension Adjustment

The same procedure will be performed for the dimension $L_2$, that is, the crank length, which is considered a fundamental dimension in the linkage. The different variations are:

- $L_2 - 15\ mm$
- $L_2 - 2\ mm$

Due to the positive results, no more variations will be studied (Fig. 6. 2):

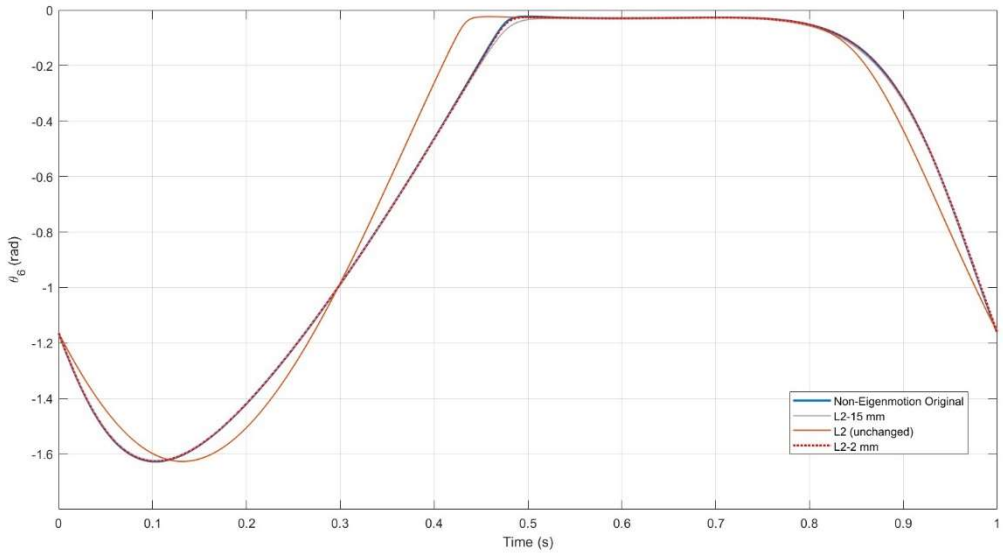


**Fig. 6. 2**: Output motions of the mechanism for different variations of the dimensional parameter $\boldsymbol{L_2}$, along with those of the mechanism with its original dimensions before and after the application of Eigenmotion.

It can be seen on how the output motion curve for $(L_2 - 2\ mm)$, shown as discontinuous and red in Fig. 6. 2, fits the original motion very accurately. If attempted for $L_2 - 1\ mm$, the resulting motion no longer fits the desired one, therefore $(L_2 - 2\ mm)$ is considered as the best variation.

This would indicate that, adjusting this dimension and using the same mechanism with a two-millimeter shorter crank link, its resulting motion would fit the desired one with a satisfactory accuracy when operating in Eigenmotion. Therefore, this adjusted mechanism could perform its desired tasks for industrial processes with a high accuracy while increasing their energy efficiency. This mentioned accuracy can be better seen in Fig. 6. 3:

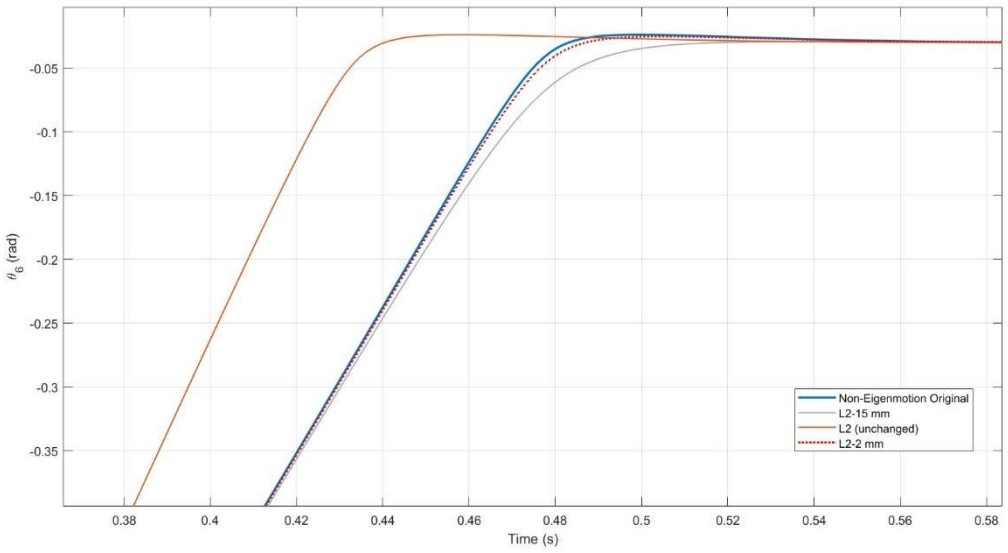


**Fig. 6. 3**: Detail from Fig. 6. 2, where the level of improvement in the output motion for ($\boldsymbol{L_2 - 2\ mm}$) (in discontinuous red) in comparison to its original dimensions (brown) can be seen.

This measure is considered optimal and adopted as the final solution. Therefore, the final dimensions for the 6-bar dwell linkage would be:

**Tab. 6. 1: Final Dimensional Parameters of the 6-bar Linkage for optimal output motion**

| Link | Dimension/Sub-dimensions | Joints | Length (mm) |
|---|---|---|---|
| 2 | $L_2$ | $O_2 - A$ | 537,95 |
| 3 | $L_{3,1}$ | $A - B$ | 849,83 |
| | $L_{3,2}$ | $A - C$ | 581,33 |
| 5 | $L_5$ | $C - D$ | 1046,09 |
| 6 | $L_{6,1}$ | $D - O_6$ | 789,30 |
| | $L_{6,2}$ | $O_6 - E$ | 789,30 |
| 4 | $L_4$ | $B - O_4$ | 1280,47 |
| 1 | $L_1$ | $O_2 - O_4$ | 1348,99 |

Where the coordinates of the fixed joints $O_2 - O_4 - O_6$ would remain the same as in Tab. 4.1.

## 6.3 Comparison between adjusted and original linkage

Once the dimensions of the adjusted linkage are obtained, it can be represented and compared to the original, non-adjusted linkage. Fig. 6.4. (a) shows the adjusted linkage in its "maximum dyad displacement" position, the same as the original linkage in Fig. 5. 1.. Due to the dimensional differences, the angles $\theta_3, \theta_4, \theta_5, \theta_6$ differ from those in the original linkage.

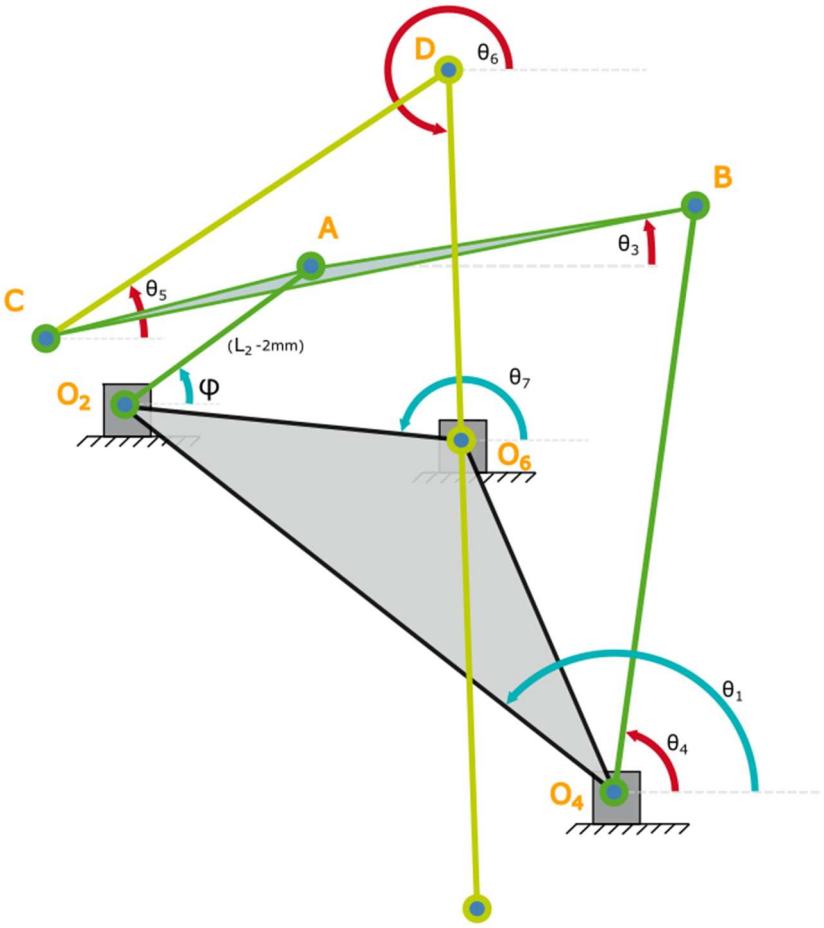


(a) **Adjusted dwell linkage, in the same position as the original original linkage in Fig. 5.1. The link angles that differ from the original are in red.**

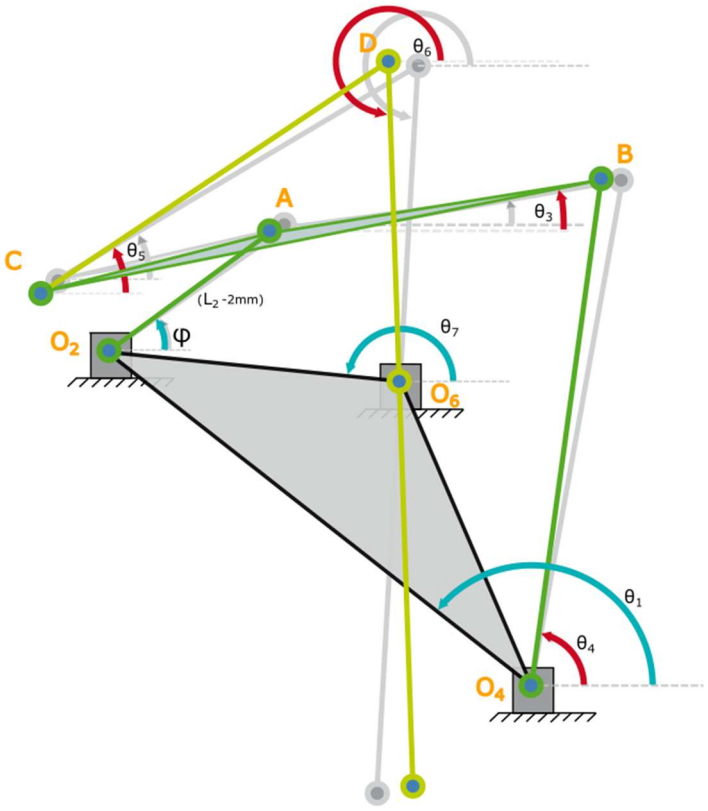


(b) **Superposition of the original and adjusted linkages, where the different link angles (in red) for the same position (*φ*) can be seen.**

**Fig. 6. 4**: Representation of the adjusted dwell linkage (a) and comparison of the adjusted linkage to the original (b).

The difference between the angles can be better seen in Figure 6. 4 (b), which shows an overlay of the adjusted linkage and the original, non-adjusted one.

# 7 Summary

This thesis was undertaken to study the relationship between dwell mechanisms and Eigenmotion.

Its first aim was to gain a better understanding of both topics. For this purpose, an accessible introduction to Eigenmotion and dwell mechanisms has been outlined respectively. Literature research on dwell mechanisms has been conducted and a systematized display of dwell mechanisms has been presented, classifying them according to their different motions and working principles. An exhaustive evaluation of the advantages and disadvantages of the use of cams and linkages has been made. In the interest of conducting a more feasible study of Eigenmotion for the dwell mechanism, dwell linkages have been chosen.

A visual assembly of different examples of dwell linkages for each dwell motion type has been carried out. A significant finding is the influential role of coupler curves in dwell linkages, which are essential to define and allow not only their motion geometry (as straight-line or arc dwells), but also their different dwell parameters (as the duration of the dwell in the crank rotation). The H&N Atlas of Coupler Curves is considered an indispensable finding, both to the classification of dwell motions and to the design of original dwell linkages.

The second aim of this thesis was to design an original dwell mechanism and evaluate the feasibility of studying its performance in Eigenmotion. To this end, an overview of different dwell linkage design methods has been conducted, including accessible step-by-step explanations along with visual materials. After evaluating the possible methods, the one considered as the most useful and precise has been chosen and successfully implemented. The simulation and dimensioning of the dwell linkage have been carried out using IGMR planar mechanism software Mechdev. A kinematic analysis of the designed dwell linkage has been conducted, dividing it into two sub-chains, and taking geometrical differences in the simulated coupler link into account. Eigenmotion has been calculated and simulated using MATLAB.

An offset between the pre- and post-Eigenmotion resulting motions has been noticed. Therefore, a dimensional adjustment of the dwell linkage has been performed in order to obtain a more fitting output motion. Slight variations in the crank length have led to very accurately fitting output motions for the dwell linkage operating in Eigenmotion. The final dimensions of the linkage as well as the coordinates of its fixed joints have been presented.

# 8 Outlook

The results of this thesis support previous research into relationships between dwell mechanisms and Eigenmotion.

In the initial study on the topic of dwell mechanisms, a difficulty was found regarding fragmented information on the topic. A clear outline of dwell mechanism types, working principles and practical applications was not found easily. This thesis provides an accessible and thorough insight into the implementation of dwell mechanisms, gathering their different industrial applications, main types, and advantages and disadvantages to their implementation. A more specialized study has been conducted on dwell linkages, which leaves the topic of cams at a more introductory level. This thesis lays the groundwork for future research into the design energy efficient dwell linkages using Eigenmotion.

This study was limited in the absence of algorithm implementation, since only a dimensional adjustment was carried out on the linkage to improve its output motion.

The scope of the study was also limited in terms of practical applications for the designed dwell linkage. A specific industrial function was not found to build the design of the linkage around. This initial step would complete the full process of dwell linkage design. A natural progression of this work would be to analyze how to draw specific desired dwell motions out of an industrial process requirement, so that the designed linkage can perform specific practical functions. This could be done by obtaining an approximate coupler curve geometry from the required process motion and comparing it to the diverse coupler curve geometries in the H&N Atlas of Coupler Curves, perhaps by overlaying. Further research in this field could lead to the creation of a systematized dwell linkage design method for industrial processes.

Taken together, the findings of this thesis support strong recommendations to further study the relationships between dwell mechanisms and Eigenmotion.

## Bibliography

[Cal08] Callesen, M.
*Der Antrieb ungleichmäßig übersetzender Getriebe durch Motion-Control-Systeme*, Nutzungsaspekte Betriebsverhalten und Bewegungsoptimierung, Düsseldorf: VDI-Verl., Als Ms. gedr, 2008, ISBN 978-3-18-514608-4.

[CLN02] Cardona, A.; Lens, E.; Nigro, N.,
Optimal Design of Cams. In: Multibody System Dynamics,
Netherlands: Kluwer Academic Publishers, 2002, pp. 285–305.

[EC16] European Commission Outcome of the October 2014 European Council, Framework for Climate & Energy, 2016.
https://climate.ec.europa.eu/system/files/2016-11/2030_euco_conclusions_en.pdf
(Last checked on 28/08/2023)

[Eur12] European Union Richtlinie 2012/27/EU des europäischen Parlaments und des Rates vom 25. Oktober 2012 zur Energieeffizienz, zur Änderung der Richtlinien 2009/125/EG und 2010/30/EU und zur Aufhebung der Richtlinien 2004/8/EG und 2006/32/EG, 2012/27/EU, 2012.

[HN99] A. Hrones, J.; L. Nelson, G.
*Analysis of the Four-Bar Linkage*, its Application to the Synthesis of Mechanisms.
New York: The Technology Press of the Massachusetts Institute of Technology and John Wiley & Sons, Inc., 1951, ISBN 9780262080033

[KCH15] Kerle, H.; Corves, B; Hüsing, M.
*Getriebetechnik*, Grundlagen, Entwicklung und Anwendung ungleichmässig übersetzender Getriebe, 5. Auflage. Wiesbaden: Springer Fachmedien Wiesbaden, 2015, ISBN 9783658100568

[KP98] Kyoto Protocol to the United Nations Framework Convention on Climate Change, United Nations, 1998. https://unfccc.int/resource/docs/convkp/kpeng.pdf
(Last checked on 28/08/2023)

[MPR07] McKane, A.; Prince, L.; de la Rue du Can, S.
Policies for Promoting Industrial Energy Efficiency in Developing Countries and Transition Economies. In: Sustainable Industrial Development, Commission for Sustainable Development, 2007.

[Nor99] Norton, R. L.
*Design of* Machinery, an Introduction to the Synthesis and Analysis of Mechanisms and Machines, Second Edition.
Worcester, Massachusetts: McGraw-Hill, 1999, ISBN 0-07-048395-7

[SC18] Schwarzfischer, F.; Corves, B.
The Dynamic Synthesis of an Energy-Efficient Watt-II-Mechanism
Conference Paper, October 2018, DOI: 10.1007/978-3-319-67567-1_20

[Schwa19] Schwarzfischer, F.
Energieeffiziente Bewegungssysteme durch Nutzung der Eigenbewegung
Doctorate Dissertation, Faculty of Mechanical Engineering, RWTH Aachen, January 9th 2019,

[SHC17] Schwarzfischer, F.; Hüsing, M.; Corves, B.
The Dynamic Synthesis of an Energy-Efficient Slider-Crank-Mechanism
Proceedings of the International Symposium of Mechanism and Machine Science, 2017 AzCIFToMM – Azerbaijan Technical University 11-14 September 2017, Baku, Azerbaijan

[SHC18] Schwarzfischer, F.; Hüsing, M.; Corves, B.
Dynamic synthesis of energy-efficient mechanisms
Int. J. Mechanisms and Robotic Systems, Vol. 4, No. 4, Pgs. 401-417, 2018

[SE84] Sandor, G. N.; Erdman, A. G.
*Mechanism Design*, Analysis and Synthesis, Vol. 2.
New Jersey: Prentice-Hall, INC., 1984, ISBN 0130114375

[Sta23] German Federal Statistical Office (Statistisches Bundesamt)
Energy Consumption
https://www.destatis.de/DE/Themen/Branchen-Unternehmen/Energie/Verwendung/_inhalt.html
(Last checked on 28/08/2023)

[Sto05] Stolle, G.,
Verfahren zur Maßsynthese sechs- und achtgliedriger ebener Gliedführungs- und Übertragungsgetriebe, Aachen: Shaker Verlag, 2005, ISBN 3-8322-3889-1.

[SWB09] Schröter, M.; Weißfloch, U.; Buschak, D.
Energieeffizienz in der Produktion - Wunsch oder Wirklichkeit?,
Energieeinsparpotentiale und Verbreitungsgrad energieeffizienter Techniken,
Fraunhofer ISI: Modernisierung der Produktion.
Mitteilungen aus der ISI-Erhebung (Nr. 51), 2009

[Tor04] Torfason, L. E.
*A Thesaurus of Mechanisms*, in *Standard Handbook of Machine Design,* Third Edition, Part 1, Chap. 2.
edited by J. E. Shigley and C. R. Mischke. New York: McGraw-Hill, 2004, ISBN 9780071441643

[UPS17] Uicker, Jr, J. J.; Pennock, G. R.; Shigley, J. E.
*Theory of Machines and Mechanisms*, Fifth Edition.
New York: Oxford University Press, 2017, ISBN 9780190264482

## List of figures

## List of tables

## Appendix A: Design of a single arc six-bar dwell linkage using graphic method

In this annex, the original transparent sheet with the graphic design of the self-made dwell linkage is displayed, as mentioned in Section 3.

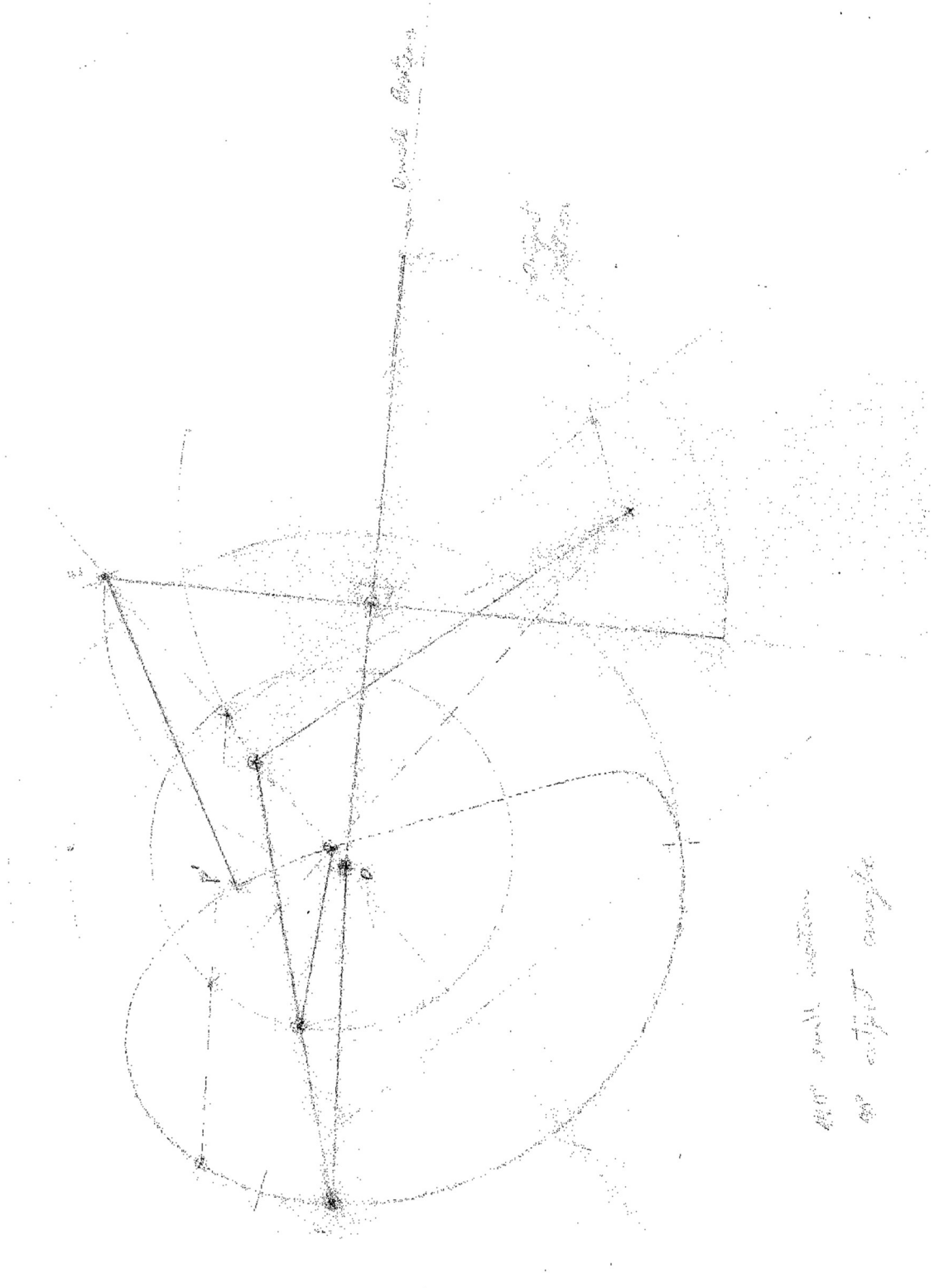

## Appendix B: MatLab Codes

- 1st File: "position4b.m"

```
%4 bar sub chain position equations: Theta 3, Theta 4

function F = position4b(theta34,phi)


% Input crank angle (degree of freedom)

%phi = 172.9*pi/180;


% Parameters (constants)

L2 = 539.949;

L31 = 849.826;

L4 = 1280.4704;

L1 = 1348.9946;

theta1 = 141.8*pi/180;


% Left part of equations: Position equations for 4-bar subchain


F(1) = L2*cos(phi) + L31*cos(theta34(1)) - L4*cos(theta34(2)) + L1*cos(theta1);


F(2) = L2*sin(phi) + L31*sin(theta34(1)) - L4*sin(theta34(2)) + L1*sin(theta1);


end
```

- 2nd File: "positiondyad.m"

```
%dyad sub chain position equations: Theta 5, Theta 6

function F = positiondyad(theta56,phitheta3)




% Parameters (constants)

L2 = 539.949;

theta7 = 3.0412;

L32 = 581.329;

L5 = 1046.093;

L61 = 789.297;

L7 = 737.181;

alpha = 0.078294164348430;

%%

%

theta3 = phitheta3(2);

phi = phitheta3(1);




% Left part of equations: Position equations for dyad subchain


F(1) = L2*cos(phi) + L32*cos(theta3-pi+alpha) + L7*cos(theta7) + L61*cos(theta56(2))
+ L5*cos(theta56(1));


F(2) = L2*sin(phi) + L32*sin(theta3-pi+alpha) + L7*sin(theta7) + L61*sin(theta56(2))
+ L5*sin(theta56(1));


end
```

- 3rd File: "energykin.m"

```
function Ekin = energykin(phi,phidot,theta3,dtheta3dphi,theta4,dtheta4dphi,theta5,dtheta5dphi,theta6,dtheta6dphi)

rho = 2.7e-1; % Aluminum length density: 2.7g/cm3 (rho = 0.27 Kg/cm2/m)


% Lengths (m)

L1 = (1348.9946)/1000;

L2 = 539.949/1000;

L31 = 849.826/1000;

L32 = 581.329/1000;

L4 = 1280.4704/1000;

L5 = 1046.093/1000;

L61 = 789.297/1000;

L62 = L61/1000;

L7 = 737.181/1000;


% Fixed points coordinates (m)

xO4 = 1060.14/1000;

yO4 = -834.2/1000;


xO6 = 733.47/1000;

yO6 = -73.88/1000;


% Fixed angles (rad)

theta1 = 141.8*pi/180;

theta7 = 3.0412;

alpha = 0.078294164348430;
```

```
xA = L2*cos(phi); xAdot = -L2*sin(phi)*phidot;

yA = L2*sin(phi); yAdot = L2*cos(phi)*phidot;


xB = xA + L31*cos(theta3); xBdot = xAdot - L31*sin(theta3)*dtheta3dphi*phidot;

yB = yA + L31*sin(theta3); yBdot = yAdot + L31*cos(theta3)*dtheta3dphi*phidot;


xC = xA + L32*cos(theta3-pi+alpha); xCdot = xAdot - L32*sin(theta3-
pi+alpha)*dtheta3dphi*phidot;

yC = yA + L32*sin(theta3-pi+alpha); yCdot = yAdot + L32*cos(theta3-
pi+alpha)*dtheta3dphi*phidot;


xD = xC + L5*cos(theta5+pi); xDdot = xCdot - L5*sin(theta5+pi)*dtheta5dphi*phidot;

yD = yC + L5*sin(theta5+pi); yDdot = yCdot + L5*cos(theta5+pi)*dtheta5dphi*phidot;


% #2 (O2A - section: 1 cm2)

m2 = rho*L2;

J2 = (m2*L2^2)/3;


xcm2 = xA/2; xcm2dot = xAdot/2;

ycm2 = yA/2; ycm2dot = yAdot/2;

vcm2 = sqrt(xcm2dot^2 + ycm2dot^2);


% #3 (Triangle ABC - it is aproximates a a bar with section 1 cm2)

m3 = rho*(L31+L32);

J3 = (m3*(L31+L32)^2)/12 + m3*((xA - (xB+xC)/2)^2 + (yA - (yB+yC)/2)^2);


xcm3 = (xA + xB + xC)/3; xcm3dot = (xAdot + xBdot + xCdot)/3;

ycm3 = (yA + yB + yC)/3; ycm3dot = (yAdot + yBdot + yCdot)/3;

vcm3 = sqrt(xcm3dot^2 + ycm3dot^2);
```

```
% #4 (O4B - section: 1 cm2)

m4 = rho*L4;

J4 = (m4*L4^2)/3;


xcm4 = xO4 + (L4/2)*cos(theta4); xcm4dot = -0.5*L4*sin(theta4)*dtheta4dphi*phidot;

xcm4 = yO4 + (L4/2)*sin(theta4); ycm4dot = 0.5*L4*cos(theta4)*dtheta4dphi*phidot;

vcm4 = sqrt(xcm4dot^2 + ycm4dot^2);


% #5 (CD - section: 1 cm2)

m5 = rho*L5;

J5 = (m5*L5^2)/3;


xcm5 = (xC + xD)/2; xcm5dot = (xCdot + xDdot)/2;

ycm5 = (yC + yD)/2; ycm5dot = (yCdot + yDdot)/2;

vcm5 = sqrt(xcm5dot^2 + ycm5dot^2);


% #6 (- section 1 cm2)

m6 = rho*(L61+L62);

J6 = (m6*(L61+L62)^2)/12;


% Kinetic energy

EkinT = (m2*vcm2^2 + m3*vcm3^2 + m4*vcm4^2 + m5*vcm5^2)/2;


EkinR = (J2*phidot^2 + J3*(dtheta3dphi*phidot)^2 + J4*(dtheta4dphi*phidot)^2 +
J5*(dtheta5dphi*phidot)^2 + J6*(dtheta6dphi*phidot)^2)/2;


Ekin = EkinT + EkinR;


end
```

- 4th File: "kinematicsEigen.m"

```
clear all

%Array vorbereiten

phistep = 0.01;

h = round(2*pi/phistep);

X = cell(h,0);

Y = cell(h,0);

S = cell(h,0);

phi_0 = 0;

phidot_0 = 0.7;


 % Angles computation for phi: theta3, theta4, theta5, theta6

theta340 = [0,0];

theta560 = [0,0];


c = 0;


for phi=0:phistep:2*pi

    c = c+1;

    optionsfsolve = optimoptions('fsolve','OptimalityTolerance',1e-6);

    fun1 = @(theta34)position4b(theta34,phi);

    theta34 = fsolve(fun1,theta340,optionsfsolve); %

    theta3(c)= theta34(1);

    theta4(c)= theta34(2);


    fun2 = @(theta56)positiondyad(theta56,[phi,theta3(c)]);

    theta56 = fsolve(fun2,theta560,optionsfsolve); %

    theta5(c)= theta56(1);

    theta6(c)= theta56(2);
```

```
    theta560 = [theta5(c),theta6(c)];


end
% Angles derivatives computation: dtheta3dphi = d(theta3)/d(phi), ...
phidot = 2*pi; % It is a scalar!


dtheta3dphi = diff(theta3)/phistep;
dtheta3dphi = [dtheta3dphi(1),dtheta3dphi];


dtheta4dphi = diff(theta4)/phistep;
dtheta4dphi = [dtheta4dphi(1),dtheta4dphi];


dtheta5dphi = diff(theta5)/phistep;
dtheta5dphi = [dtheta5dphi(1),dtheta5dphi];


dtheta6dphi = diff(theta6)/phistep;
dtheta6dphi = [dtheta6dphi(1),dtheta6dphi];


% Kinetic energy-Jred
% Ekin_0 = Ekin_0 (phidot_0=1) * phidot_0^2
c = 0;
for phi=0:0.01:2*pi
    c = c+1;
    Ekin =
energykin(phi,phidot,theta3(c),dtheta3dphi(c),theta4(c),dtheta4dphi(c),theta5(c),d
theta5dphi(c),theta6(c),dtheta6dphi(c));
    Jred = 2*Ekin/phidot^2;


    Ekin_0 =
energykin(phi_0,phidot_0,theta3(1),dtheta3dphi(1),theta4(1),dtheta4dphi(1),theta5(
1),dtheta5dphi(1),theta6(1),dtheta6dphi(1));
```

```
    Jred_0 = 2*Ekin_0/phidot_0^2;


    omega_e = phidot_0*sqrt(Jred_0)/sqrt(Jred);


    X{c} = phi;
    Y{c} = 1/omega_e;
    S{c} = Ekin;
end
%Ausgabe:
Xv = cell2mat(X);
Yv = cell2mat(Y);
Sv = cell2mat(S);


Q = cumtrapz(Xv,Yv);
Qend = Q(end);


phi_e = Q/Q(end);


%figure
%plot(Xv/(2*pi),Xv,phi_e, Xv);
%grid on;
figure
plot(Xv/(2*pi),theta6,phi_e,theta6)
grid on;


load original
figure
plot(toriginal,theta6original,phi_e,theta6)
grid on;
```